SINGLE-TRIAL ANALYSIS AND ITS APPLICATIONS IN EEG AND SIMULTANEOUS EEG-FMRI STUDIES

By

YUELU LIU

A DISSERTATION PRESENTED TO THE GRADUATE SCHOOL
OF THE UNIVERSITY OF FLORIDA IN PARTIAL FULFILLMENT
OF THE REQUIREMENTS FOR THE DEGREE OF
DOCTOR OF PHILOSOPHY

UNIVERSITY OF FLORIDA

2013

To my Mom and Dad, and my wife, Bing
For their love and support

ACKNOWLEDGMENTS

First and foremost, I would like to express my deepest appreciation to my advisor, Dr. Mingzhou Ding, for his continuous support and patience in guiding me through the toughness of my research. His academic excellence, wisdom, and sharpness set as an invaluable exemplar for me to emulate. I owe him a tremendous amount of gratitude for introducing me into the exciting realm of cognitive neuroscience research and providing me with the opportunity to conduct highest-quality research. My past five years spent working with him have been exceptionally rewarding yet at the same time full of fun and excitement.

I would like to express my special thanks to Dr. Andreas Keil, for his constant encouragement and guidance and with whom I had the honor and pleasure to collaborate for the most part of my stay at UF. His enthusiasm and professionalism have influenced profoundly my career development. Also, many thanks to my committee members, Drs. Bruce Wheeler and Hans van Oostrom for their insightful comments and constructive suggestions throughout various stages of my research and dissertation preparation.

I would like to thank Dr. Andrew Ahn for introducing me to the field of clinical translational research and giving me the opportunity to participate in cutting-edge clinical studies. I am also grateful of Dr. Peter Lang, Dr. Margaret Bradley, Dr. George Mangun at UC Davis, Dr. Robert Knight at UC Berkeley, Dr. Yang Jiang at U of Kentucky, and Dr. Onur Seref at Virginia Tech for the inspiring discussions that facilitated immensely my research and manuscript writing. I am thankful of Vladimir Miskovic, Vincent Costa, Jesse Bengson at UC Davis, and Bradley Voytek at UCSF for

their timely assistance and professional knowledge that helped me overcome obstacles in my research.

Special thanks to Haiqing Huang, who has helped me diligently in carrying out all the lengthy experiments throughout the past few years. Also, special thanks to Rajasimhan Rajagovindan for his insightful comments during the early days of my research and for our fun discussions just about everything. I want to express my big thanks to all former and current lab colleagues: Yan Zhang, Anil Bollimunta, Yonghong Chen, Sahng-Min Han, Kristopher Anderson, Xiaotong Wen, Jue Mo, Chao Wang, Amy Trongnetrpunya, Yijun Zhu, Siyang Yin, Felix Bartsch, Abhijit Rajan, and Immanuel Babu Henry Samuel. Thank you all for the motivating discussions and also for being my best friends.

Thanks to all BME staffs including Tifiny McDonald, Katherine Whitesides, Diana Dampier, Art Bautista-Hardman, Ruth McFetridge, Valerie Anderson, and Todd Andersen-Davis. My research and life here in the BME department could not have been easier all because of your support and assistance in handling the daunting paper works and computer-related issues.

Above all, I want to express my heartfelt appreciation to my parents, and most importantly, my wife Bing. Your understanding and support have been the everlasting power source that stimulates me to advance forward. My achievement could not have been attained without your unconditional love and sacrifices.

TABLE OF CONTENTS

Page

ACKNOWLEDGMENTS 4

LIST OF TABLES 8

LIST OF FIGURES 9

ABSTRACT 10

CHAPTER

1 INTRODUCTION 12

2 EFFECTS OF EMOTIONAL CONDITIONING ON EARLY VISUAL PROCESSING: TEMPORAL DYNAMICS REVEALED BY ERP SINGLE-TRIAL ANALYSIS 20

2.1 Background and Significance 20
2.2 Materials and Methods 22
2.2.1 Participants 22
2.2.2 Stimuli 23
2.2.3 Paradigm 24
2.2.4 Data Acquisition 25
2.2.5 ASEO Single-trial Analysis 26
2.3 Results 29
2.3.1 Average ERP Analysis 29
2.3.2 Single-trial Estimation of ERPs 30
2.3.3 Temporal Dynamics of the P1 Component 30
2.4 Discussion 32

3 NEURAL SUBSTRATES OF THE LATE POSITIVE POTENTIAL IN EMOTIONAL PROCESSING 43

3.1 Background and Significance 43
3.2 Methods 45
3.2.1 Participants 45
3.2.2 Stimuli and Procedure 45
3.2.3 Simultaneous EEG-fMRI Acquisition 47
3.2.4 EEG Data Preprocessing 48
3.2.5 Single-trial Estimation of LPP 49
3.2.6 MRI Data Analysis 50
3.3 Results 52
3.3.1 ERP Analysis 52
3.3.2 fMRI Analysis 54
3.3.3 Trial-by-trial Coupling of LPP and BOLD 55
3.4 Discussion 56

3.4.1 Methodological Considerations 56
3.4.2 LPP-BOLD Coupling and Its Theoretical Significance 57
3.4.3 Category-specific Network Processing 59

4 MODULATION OF ALPHA OSCILLATIONS IN ANTICIPATORY VISUAL ATTENTION: CONTROL STRUCTURES REVEALED BY SIMULTANEOUS FMRI-EEG 69

4.1 Background and Significance 69
4.2 Materials and Methods 70
4.2.1 Participants 70
4.2.2 Paradigm 71
4.2.3 EEG Data Acquisition and Preprocessing 72
4.2.4 fMRI Acquisition and Preprocessing 74
4.2.5 EEG Spectral Analysis 75
4.2.6 EEG-informed fMRI Analysis 76
4.3 Results 77
4.3.1 Attentional Modulation of Alpha 78
4.3.2 BOLD Activations Evoked by the Cue 78
4.3.3 BOLD-Alpha Coupling: Negative Correlations 78
4.3.4 BOLD-Alpha Coupling: Positive Correlations 79
4.3.5 Coupling between Alpha Lateralization Index and BOLD 79
4.4 Discussion 80
4.4.1 Alpha and Dorsal Attention Network 80
4.4.2 Alpha and Task-Irrelevant Networks 82
4.4.3 Differential Roles of IPS and FEF in Controlling Alpha 83
4.4.4 The Role of dACC in Anticipatory Visual Attention 83
4.4.5 Summary 84

5 CONCLUSIONS 91

LIST OF REFERENCES 95

BIOGRAPHICAL SKETCH 111

LIST OF TABLES

Table		Page
2-1	Results from MARS piecewise linear regression analysis	39
3-1	Regions showing coupling between LPP amplitude and BOLD	63
4-1	Event-related activations following cue onset	85
4-2	Coupling between alpha and BOLD with attend left and right combined	86

LIST OF FIGURES

Figure		Page
2-1	Schematic of paradigm and ERP	39
2-2	Temporal distribution of trials analyzed in this study	40
2-3	Illustration of ASEO single-trial analysis on a representative subject	41
2-4	Smoothing of single-trial ERPs	41
2-5	Temporal dynamics of P1 amplitude	42
3-1	ERP analysis	64
3-2	Single-trial ERP analysis	65
3-3	Single-trial LPP dynamics	66
3-4	Activation maps based on BOLD contrast	67
3-5	LPP-BOLD coupling maps	68
4-1	An illustration of the sequence of events within a trial	87
4-2	Attentional modulation of alpha power and BOLD	88
4-3	Negative coupling between BOLD and alpha with Attend Left and Right combined	89
4-4	Positive coupling between BOLD and alpha with Attend Left and Right combined.	90
4-5	Coupling between BOLD and alpha lateralization index	90

Abstract of Dissertation Presented to the Graduate School
of the University of Florida in Partial Fulfillment of the
Requirements for the Degree of Doctor of Philosophy

SINGLE-TRIAL ANALYSIS AND ITS APPLICATIONS IN EEG AND SIMULTANEOUS EEG-FMRI STUDIES

By

Yuelu Liu

August 2013

Chair: Mingzhou Ding
Major: Biomedical Engineering

Electrophysiological recordings such as human electroencephalogram (EEG) and monkey local field potentials (LFP) are traditionally thought to be comprised of a deterministic event-related potential (ERP) plus a task-irrelevant random noise. However, evidence has long suggested that the ERP waveform can vary from trial to trial. Such trial-to-trial variability often bears important information about the dynamics of the underlying cognitive processes. With recent advancements in single-trial analysis methods, we seek to explore in this dissertation the dynamics of cognitive processes underlying higher-level cognitive functions including visual attention, emotional processing, and classical conditioning.

First, we applied a recently developed single-trial analysis method, Analysis of Single-trial ERP and Ongoing signals (ASEO), to study the trial-to-trial temporal dynamics of sensory facilitation during classical aversive conditioning. Estimating the amplitude of the P1 component elicited by the conditioned stimuli (CSs), we found that P1 amplitude fluctuations within the acquisition session followed three distinct phases. Further, the effects of sensory facilitation toward the CS predicting aversive outcomes, compared to the CS predicting neutral outcomes, were manifested by differences in the

rate of P1 amplitude changes within each phase. Second, we investigated brain structures involved in the generation and modulation of the late positive potential (LPP) during emotional processing. Correlating single-trial LPP amplitude with the simultaneously recorded blood-oxygen-level-dependent (BOLD) activity, we found that regions contributing to scalp-recorded LPP included the visual cortices and emotional processing structures. Moreover, the degree of contribution to scalp LPP from these structures was valence specific. Finally, we investigated brain areas contributing to the attentional modulation of alpha (8–12 Hz) in spatial visual attention. Our results suggest that the intraparietal sulcus, a core region within the frontoparietal attention network, modulates the trial-to-trial alpha desynchronization. Further, we found a positive correlation between alpha lateralization and BOLD in dorsal anterior cingulate cortex (dACC), suggesting a role for dACC in facilitating the attentional set via executive influences over attentional control systems.

In conclusion, the results suggest that trial-to-trial variability is an important aspect of the cognitive process. Exploring such variability can gain us valuable insights into the neuronal mechanisms of higher-level cognitive processes.

CHAPTER 1
INTRODUCTION

Studies of brain functions by electroencephalogram (EEG) or local field potentials (LFPs) often rely on averaging over a large number of repeated experimental trials to enhance the signal-to-noise ratio (SNR). This is usually performed by aligning all trial epochs belonging to a certain experimental condition to the onset of an event and then computing an ensemble average across all epochs. The resulting time series, the averaged event-related potential (AERP), is an estimate of the true underlying event-related potential (ERP) and has been the major tool for neuroscientists to explore basic brain functions (Luck, 2005). The underlying assumption for this ensemble averaging procedure is that the recorded neural signal following experimental events can be modeled as a linear combination of the ERP and an ongoing activity. The ERP is assumed to be deterministic and does not vary across trials, whereas the ongoing activity is treated as task-irrelevant brain activities. However, evidence has long suggested that the ERP can take distinct waveforms across experimental trials and such trial-to-trial variability has been demonstrated to relate to fluctuations in performances as well as cognitive processes (Woody, 1967; Coppola et al., 1978; Truccolo et al., 2002, 2003; Chen et al., 2006; Knuth et al., 2006; Truccolo et al., 2003). Moreover, the ongoing activity is not task-irrelevant and has been shown to contain rich information about neuronal oscillations also closely related to cognitive functions (Keil et al., 2007; Klimesch et al., 2007; Anderson and Ding, 2011; Rajagovindan and Ding, 2011; Wang and Ding, 2011). Simply taking the ensemble average as the estimator for the ERP would potentially smooth out such trial-to-trial information of the underlying cognitive processes and thereby rendering the AERP a suboptimal estimator. Thus, it is

important that researchers utilize single-trial analysis methods to reduce the level of information deterioration involved in traditional ensemble averaging.

The advantage of adopting single-trial analysis to examine cognitive functions can be summarized in the following three aspects. In the first place, single-trial ERP estimation allows one to better reconstruct the AERP. In the traditional ensemble averaging approach, trial-to-trial variability negatively impacts the SNR of the estimated AERP as the latency shift for a given ERP component tends to decrease the estimated amplitude and widen the waveform after the averaging procedure. Estimating and accounting for the trial-to-trial latency shift in single-trial ERPs prior to the ensemble averaging can therefore reduce the temporal smearing effect and enhance the SNR of the AERP.

Second, single-trial analysis allows the study of cognitive functions via trial-to-trial variability. Fluctuations in single-trial ERP amplitudes and latency shifts often contain important information about the cognitive processes such as attention (Anderson and Ding, 2011; Rajagovindan and Ding, 2011; Zhang and Ding, 2010), working memory (Anderson et al., 2010), conflict monitoring (Debener et al., 2005), and associative learning (Keil et al., 2007). Hence, by studying such task-related trial-to-trial variability, one can gain additional information about the dynamics of neuronal mechanisms that cannot be obtained by the traditional ensemble averaging approach. In fact, single-trial ERP analysis has been an indispensable component in simultaneous EEG and functional magnetic resonance imaging (fMRI) analysis (Eichele et al., 2005; Debener et al., 2005, 2007; Bénar et al., 2007).

Third, estimating single-trial ERP allows better estimation of the ongoing activity (Wang et al., 2008; Xu et al., 2009). The ongoing activity is usually estimated by subtracting the AERP from the original data. Yet, recent evidence suggests that this simple subtraction scheme might not be sufficient to remove the ERP due to the trial-to-trial variability in the ERP time series (Wang et al., 2008). The residual ERP in the estimated ongoing activity can cause spurious results when one attempts to analyze properties of the ongoing activity, leading to erroneous interpretations. Single-trial analysis can reduce the level of residual ERP in the estimated ongoing activity when one adjusts for trial-to-trial variability in the ERP and subtracts the estimated single-trial ERP from each corresponding trial. This alternative approach has been shown to give better estimations of the ongoing activity and is effective in reducing spurious functional connectivity (Wang et al., 2008).

A number of single-trial analysis methods have emerged in the past decade. These methods involve the use of maximum-likelihood estimation (McGillem et al., 1985; Tuan et al., 1987; Lange et al., 1997; Jaskowski and Verleger, 1999), wavelet denoising (Bartnik et al., 1992; Quiroga, 2000; Quiroga and Garcia, 2003), Bayesian estimation (Truccolo et al., 2003), and other iterative methods (Xu et al., 2009). In particular, an iterative algorithm called “Analysis of Single-trial ERP and Ongoing signal (ASEO; Xu et al., 2009)” has been shown to achieve a relative high performance level. The ASEO algorithm assumes that the recorded LFP or EEG activity following event onset can be described by a Variable Signal Plus Ongoing Activity (VSPOA) model (Chen et al., 2006). This signal generative model assumes that the ERP can be decomposed into a set of time-domain components, where each component has a fixed waveform but could

vary in its amplitude and latency across trials. The ongoing activity is further modeled as an autoregressive (AR) model which gives a realistic description of the brain's oscillatory activities. Based on the VSPOA model, the ASEO algorithm estimates iteratively the waveforms, amplitude scaling factors, and latency shifts for each ERP components, as well as the AR coefficients for the ongoing activity. It can be shown that with this iterative estimation procedure, the ASEO algorithm can outperform other single-trial ERP estimation algorithms such as the dVCA method (Truccolo et al., 2003).

In this dissertation, the dynamics of neuronal processing underlying three important higher-level cognitive functions, i.e., classical conditioning, emotional processing, and voluntary attention, are studied via the above-mentioned ASEO single-trial analysis. Specifically, the dissertation examines these questions along the following three specific aims.

Aim 1: To investigate the detailed trial-by-trial dynamics of sensory facilitation process underlying the classical aversive conditioning. A key aspect of adaptively responding to stimuli that signify threats or rewards is the in-depth sensory analysis of such stimuli (Bradley et al., 2003). Simple neutral stimuli, when temporally paired with the emotionally-engaging unconditioned stimuli in classical conditioning paradigms, were found to evoke increased sensory responses, compared to responses elicited by the same stimuli but not paired with a noxious stimulus (Stolarova et al., 2006). Such effects of sensory facilitation were further found to increase over two consecutive sessions of conditioning, demonstrating sustained learning effects on the time scale of experimental blocks (Stolarova et al., 2006; Keil et al., 2007). Yet to date, the detailed trial-to-trial temporal dynamics of the sensory facilitation process is not known.

Understanding such detailed temporal dynamics of differential sensory changes during the associative learning process is important for both basic science problems as well as clinical translational research addressing the etiology and treatment of affective disorders (Lissek et al., 2008). For instance, reports on the habituation of the amygdala during classical conditioning (Breiter et al., 1996; Whalen et al., 1998; Buchel et al., 1999; Zald, 2003) suggest that re-entrant modulation of visual areas by amygdalo-fugal connections (Amaral and Price, 1984) decreases over time. On the other hand, mapping the trial-by-trial dynamics of emotional response is essential to characterize the dysfunctional pattern of sensory processing of phobic cues in generalized anxiety disorder (Mogg et al., 2000; Amir et al., 2009). Traditional ERP measures obtained by means of ensemble averaging do not allow for detailed information of the learning dynamics in the sensory cortex because such measures require the pooling of a substantial number of trials and thus lack trial specificity. Hence in this aim, the ASEO single-trial analysis will be employed to study the emotional experience dependent modulation of the extrastriate cortex during a classical differential conditioning paradigm. The evolving pattern of visual P1 component within a single conditioning block will be examined. I expect to observe differential temporal dynamics between the P1 amplitudes elicited by the conditioned stimuli predicting aversive (CS+) vs. neutral (CS–) emotional contents, respectively.

Aim 2: To investigate the neural substrates that contribute to the generation and modulation of the late positive potential (LPP) during emotional processing. The LPP is a reliable electrophysiological index of emotional perception in humans. During viewing of affective pictures, LPP is characterized as an amplitude enhancement in ERP starting

around 300–400 ms after picture onset for both pleasant and unpleasant stimuli, relative to the neutral stimuli. It has been shown that LPP amplitude varies systematically with the experienced intensity of the affective picture content (Schupp et al., 2000; Keil et al., 2002) and exhibits abnormal patterns in mood disorders and other psychiatric conditions (Foti et al., 2010; Leutgeb et al., 2011; Weinberg and Hajcak, 2011; Weymar et al., 2011; Jaworska et al., 2012). Despite the importance of LPP, brain structures that contribute to the generation and modulation of LPP are not well understood. Studies employing ERP source localization techniques are only partly successful because of the relatively low spatial resolution and the difficulty in resolving deep subcortical structures (Sabatinelli et al., 2007b; Keil et al., 2002).

In parallel, functional magnetic resonance imaging (fMRI) studies have found that viewing of affective pictures is associated with increased blood-oxygen-level-dependent (BOLD) activity in widespread brain regions, including occipital, parietal, inferotemporal cortices, and other higher-level emotion processing structures such as amygdala (Breiter et al., 1996; Lang et al., 1998; Bradley et al., 2003; Norris et al., 2004; Sabatinelli et al., 2005, 2009). Such extensive network activation suggests that emotionally salient contents enhance visual stimulus processing by attracting attentional and sensory processing resources (Lang et al., 1998a; Lang and Bradley, 2010). Hence, I hypothesize that if the enhanced LPP and BOLD activity during affective processing reflect a common underlying mechanism, one might expect a coupling between the LPP amplitude and BOLD activities in regions that contribute to the LPP. To test our hypothesis and identify regions that give rise to the scalp-recorded LPP, we will record simultaneous EEG-fMRI while subjects passively view emotionally arousing and neutral

pictures. Single-trial LPP amplitudes, estimated via the ASEO algorithm, will be correlated with single-trial evoked BOLD responses across the entire brain to identify brain structures contributing to the scalp-recorded LPP. Through this technique, we wish to identify structures that contribute to the LPP during processing of both pleasant and unpleasant emotions, respectively.

Aim 3: To investigate brain areas and mechanisms underlying top-down modulation of alpha oscillations (8 – 12 Hz) during spatial visual attention. A well-established phenomenon during spatial visual attention is the desynchronization of posterior alpha oscillation on the hemisphere contralateral to the direction of covert spatial attention (Worden et al., 2000; Sauseng et al., 2005; Thut et al., 2006; Rajagovindan and Ding, 2011). Such modulation of posterior alpha is thought to reflect an increase in cortical excitability among task-relevant cortices through top-down attentional mechanisms (Klimesch et al., 2007; Romei et al., 2008, 2010). Although putative sources of alpha attentional modulation have been attributed to the dorsal frontoparietal attention network as well as other higher-level executive regions (Kastner et al., 1999; Shulman et al., 1999a; Corbetta et al., 2000; Hopfinger et al., 2000; Corbetta and Shulman, 2002; Astafiev et al., 2003; Giesbrecht et al., 2003), direct evidence showing modulation of posterior alpha from these brain regions has been scarce. Further, the mechanism through which higher-order brain areas control sensory cortices to selectively enhance the processing of behaviorally relevant information and at the same time suppress the processing of behaviorally irrelevant distractors remains largely unknown. In this aim, we will address the above research questions by correlating trial-to-trial fluctuations in the posterior alpha power during the anticipatory

period with simultaneously acquired BOLD activities throughout the brain. We wish to identify separately regions associated with two forms of alpha attentional modulation, i.e., desynchronization and hemispheric lateralization. In addition, regions associated with alpha power increases will also be identified to examine potential mechanism of active inhibition over task-irrelevant networks.

CHAPTER 2
EFFECTS OF EMOTIONAL CONDITIONING ON EARLY VISUAL PROCESSING: TEMPORAL DYNAMICS REVEALED BY ERP SINGLE-TRIAL ANALYSIS

2.1 Background and Significance

Emotions, viewed in an evolutionary context, represent phylogenetically old action dispositions that facilitate survival vival of the organism and the species (Lang et al., 1998). A key aspect of adaptively responding to stimuli that signify threats or rewards is the in-depth sensory analysis of such stimuli (Bradley et al., 2003). In line with this view, neuroscience studies of emotional perception have suggested that processing of emotionally salient stimuli is facilitated at multiple stages of the visual pathway (Pizzagalli et al., 1999, 2003; Vuilleumier et al., 2001; Schupp et al., 2003, 2004). In situations that require spatial orienting to affectively arousing stimuli, studies using event-related potentials (ERPs) have shown that early visual components C1 and P1 are enhanced by affective cues (Pourtois et al., 2004). Specifically, experiments using differential classical conditioning have demonstrated increased early cortical responses over learning trials for the conditioned stimulus that predicts an unpleasant event (i.e., the CS+) across the conditioning blocks (Stolarova et al., 2006). As suggested in Keil et al. (2007), a possible explanation for such early sensory enhancement are changes in the depth-of-processing needed for discrimination, as learning progresses: Experience with a given set of stimuli and spatial locations allows observers to predict certain aspects of the stimulus array, which then no longer require in-depth processing in each subsequent trial. In terms of neural mass activity, this predictability may lead to constantly increasing cortical facilitation for a specific set of features (e.g., the orientation of the CS+ grating), at increasingly early stages of visual analysis (Stolarova et al., 2006). One prediction of this notion is that early trials should be characterized by

slower in-depth processing, followed by a successive shift of discriminant neural engagement to fewer and earlier levels of visual cortex. Changes in sensory cortices as a function of learning have been observed in experimental animals (Lee et al., 2002; Schwabe and Obermayer, 2005; Tolias et al., 2005), particularly when using intense conditioning regimens (Elbert and Heim, 2001).

Although previous work has identified the effect of learning on the time scale of experimental trial blocks, it is important for both basic science and applied questions to obtain information on the time course of differential changes during emotional learning on a trial-to-trial basis. For instance, reports on the habituation of the amygdala during classical conditioning (Breiter et al., 1996; Büchel et al., 1998, 1999b; Whalen et al., 1998; Zald, 2003) suggest that re-entrant modulation of visual areas by amygdalo-fugal connections (Amaral and Price, 1984) decreases over time. Another question of interest is the time course and duration of early visual enhancement during the first trials, as it may represent a measure of the speed of acquisition of contingencies (Moratti and Keil, 2009). Trial-by-trial dynamics of emotional learning are also an important aspect in translational research addressing the etiology, maintenance, and treatment of anxiety disorders (Lissek et al., 2008). For instance, initial hyper-vigilance and subsequent perceptual avoidance of fear-related cues may represent a dysfunctional pattern of sensory processing of phobic cues in generalized anxiety disorder, or in depression (Mogg et al., 2000), and this pattern may change over trials, e.g., with attention training (Amir et al., 2009).

ERP measures obtained by means of ensemble averaging do not allow for a detailed picture of the learning dynamics in visual cortex because they require the

pooling of a substantial number of trials and thus lack trial specificity. For instance, using ensemble averaging, Stolarova et al. (2006) examined electrocortical changes on the time scale of trial blocks, which obscures putative condition differences in terms of trial-to-trial dynamics. In this article, a novel single-trial ERP analysis method called Analysis of Single-trial ERP and Ongoing activity (ASEO) (Xu et al., 2009) is employed to study the emotional experience-dependent modulation of the extrastriate cortex during a classical differential conditioning paradigm. Treating the visual P1 component elicited by the conditioned stimuli (CS+ and CS–) as an index of early sensory processing, we estimated the amplitude of P1 on a single-trial basis over conditioning and control blocks and compared the results across the two CSs. In contrast to previous reports by Keil et al. (2007) and Stolarova et al. (2006), where block-based averaging was used, the current work aimed at examining the evolving pattern of visual P1 amplitude within a single conditioning block. Given that the P1 has been shown to be modulated by classically conditioned cues in previous studies (Pizzagalli et al., 2003; Stolarova et al., 2006), we expected to observe differential temporal dynamics between the P1 amplitudes elicited by the conditioned stimuli predicting aversive (CS+) vs. neutral (CS–) pictures, respectively.

2.2 Materials and Methods

2.2.1 Participants

Datasets from five participants (two males and three females, mean age: 22.4, SD = 1.8) were selected from an earlier study of classical emotional conditioning (Keil et al., 2007), in which 14 undergraduate students participated in exchange of class credit or a financial bonus of ~30 USD. To be selected for the single-trial analysis in the present

study, datasets had to meet the following three criteria: (a) Reliable enhancement of the eye-blink startle response measured when viewing the CS+, compared to the CS–, which was taken to index successful acquisition of contingencies (see below), (b) reliable P1 ERP scalp topography among parietal-occipital sites, and (c) excellent signal-to-noise ratio of the recorded EEG signal as indexed by a 3-dB gain between the alpha band power and power in beta and gamma band. Eight subjects showing strong contingency acquisition were included according to the first criterion. Among the eight subjects, datasets from two subjects showing abnormal P1 topography during at least one experimental condition were excluded according to criterion b). We further excluded one subject's dataset showing long segments of excessive high frequency artifact from our study. The goal of the above subject inclusion criteria was to make sure that: (1) reliable P1 temporal dynamics could be extracted from each individual subject; and (2) the P1 effects seen in the present participants would be consistent with successful conditioning as indexed by startle reflex modulation. The data from five participants meeting all three criteria were processed using the single-trial analysis technique described below.

2.2.2 Stimuli

One hundred twenty pictures from the International Affective Picture System (IAPS; Lang et al., 1997) were chosen based on their normative ratings of hedonic valence and emotional arousal as listed in the IAPS manual. The 60 unpleasant pictures contained mutilated bodies, attack scenes, and disgusting objects (mean valence: 2.2, SD = 0.6; mean arousal: 6.1, SD = 0.8). They served as the Unconditioned Stimuli (USs). The 60 neutral pictures served as control stimuli and contained landscapes, people, objects,

and abstract patterns (mean valence: 5.9, SD = 0.7; mean arousal: 3.8, SD = 0.9). The differences between these two picture categories was maximized in terms of both emotional valence and their level of emotional arousal to facilitate differential conditioning despite the relative weakness of picture USs compared to sound or electric shock stimuli used in other works. Picture USs enabled us to use rapid presentation rates, resulting in high trial counts. The affective pictures were presented centrally on a 19-in. computer monitor with a refresh rate of 70 Hz and subtended a visual angle of 7.2˚ horizontally. In addition, four types of 8-by-8 checkerboards with different colors (black and bright red, black and dark red, black and bright green, and black and dark green) were designed such that they matched the size of affective pictures. These checkerboard patterns were used to replace the affective pictures during the control block with no contingencies (see below).

Two small black and white squares (visual angle horizontally: 2.2˚) differing only in grating orientation (45˚ or 135˚) were used as CS+ and CS–, respectively. They had a spatial frequency of 2.3 cycles per degree with 100% in contrast. The gratings were presented in either the upper left or right visual field (eccentricity of the inner border: 3.58˚) prior to the affective pictures.

2.2.3 Paradigm

Two experimental blocks, a conditioning block and a control block, conducted in that order on the same day during the original experiment were analyzed in this study. The experimental timeline for the conditioning block is shown in Figure 2-1A. For each CS+ trial, the grating pattern designated as the CS+ appeared on the screen for a total of 600 ms. About 200 ms following the onset of the CS+, an affective picture was

presented centrally for a duration of 400 ms. The inter-trial interval (ITI) varied randomly between 400 and 1,400 ms (Fig. 2-1A). For each neutral trial, the grating pattern designated as the CS– was paired with the neutral and low arousing pictures in the same manner as described for the CS+. Both trial types were presented in a randomized fashion within the block. The experimental block contained a total of 480 standard trials (grating followed by an IAPS stimulus), out of which four conditions were formed, by crossing the grating orientation (CS+ versus CS–) and visual hemifield (left versus right). There were 120 trials for each condition. The experimental time line for the control block was kept the same as the conditioning block except that the affective pictures were replaced with the checkerboards mentioned above. The experiment was designed such that there was no systematic association between the grating orientation and color of checkerboard to minimize contingency reinforcement. During the experiment, participants sat at a distance of 80 cm from the computer screen. They were asked to maintain fixation of a white cross in the middle of the screen present at all times throughout recording. A chin rest was used to ensure consistency of head position and to minimize head movements.

2.2.4 Data Acquisition

The EEG was recorded using an EGI 128-channel system. The vertex (Cz) was the recording reference. The sampling rate was 250 Hz and impedances were kept below 50 kΩ as recommended by the manufacturer. Data were subjected to 0.1 Hz high-pass and 100 Hz low-pass online filtering. Artifact-free epochs (196 ms pre- and 600 ms post-stimulus interval) were obtained using the SCADS procedure suggested by (Junghöfer et al., 2000). This procedure creates distributions of statistical indices of data

quality and lets researchers identify bad channels and trials, with the latter being discarded and the former being interpolated from the full channel set. In a subsequent step, data were re-referenced to average reference. The mean number of artifact-free trials per condition was 82.

2.2.5 ASEO Single-trial Analysis

A recently developed single-trial analysis method, called Analysis of Single-trial ERP and Ongoing activity (ASEO) (Xu et al., 2009), was adopted to extract the visual single-trial ERP from the raw single trial EEG data. A detailed description of the method can be found in the above reference. Briefly, the recorded r th trial ($r = 1,2,...,R$) of the EEG data is modeled by the variable signal plus ongoing activity (VSPOA) model (Chen et al., 2006; Xu et al., 2009):

$$x_r(t) = \sum_{n=1}^{N} \beta_{rn} s_n(t - \tau_{rn}) + z_r(t) \tag{2-1}$$

where $s_n(t)$ ($n = 1,2,...,N$) is the unknown ERP component waveform with N being the total number of such components, β_{rn} and τ_{rn} are the unknown amplitude scaling factor and the latency shift for the n th ERP component, and $z_r(t)$ is the ongoing activity which is further modeled as an AR random process. With proper initial conditions, the ASEO algorithm estimates the ERP component waveforms $\{s_n(t)\}$, the corresponding single-trial amplitude scaling factors $\{\beta_{rn}\}$ and latency shifts $\{\tau_{rn}\}$, and the AR coefficients of the ongoing activity in an iterative fashion. From these estimated quantities, the single-trial event-related potentials were reconstituted, forming the basis for estimating the amplitude of the P1 component. While implementing ASEO single-trial

analysis, the number of components and the waveform for each component required by the algorithm were selected according to visual inspection of the ERP waveform for each subject. An example is illustrated in Figure 2-3C. The number of components used in this study varied from three to six. These initial components were selected according to computational considerations, and might not effectively represent the true underlying neural generating processes. Comparison of average ERPs from the raw single trial EEG time series and that from the single-trial ERPs estimated from the same raw single trial EEG time series was used to evaluate the effectiveness of the ASEO procedure (Wang and Ding, 2012; Wang et al., 2008).

The same analysis was applied to both the conditioning block and the control block. Because of the lateralized presentation of the CSs, the single-trial analysis was performed on the hemisphere contralateral to CS presentation at two lateral-posterior electrodes (channel 66 and 85 of the EGI 128-channel system) for every subject. These two electrodes, selected for exhibiting maximum ERP peak P1 amplitude, were located near sites P3 and P4 in the standard 10–20 system. Single-trial ERPs from these electrodes were estimated and reconstructed on a trial-by-trial basis for all four experimental conditions. The estimated single-trial ERPs were further subjected to a 10-trial moving averaging procedure to smooth the data and enhance signal-to-noise ratio, i.e., the 1st trial to the 10th trial were pooled together to form smoothing Bin 1 and the singletrial ERPs averaged to produce smoothed Trial 1, and the 2nd trial to the 11th trial were pooled together to form smoothing Bin 2 and the single-trial ERPs averaged to produce smoothed Trial 2, and so on. The window length for the trial-to-trial moving averaging was selected such that reliable P1 amplitude could be obtained without

compromising much trial-to-trial specificity. The time interval of the contralateral P1 component was then defined for each condition and subject, separately, and the peak voltage within the time interval was selected as the P1 amplitude measurement.

Hemispheric conditions were further combined by averaging the results over the two electrodes, leaving for comparison two experimental conditions: CS+ and CS–. To examine the effect of emotional conditioning on the CS-evoked P1 component, P1 amplitudes for CS+ and CS– conditions were averaged across five subjects, and plotted against the smoothing bin index to reveal the temporal dynamics. The temporal functions of P1 amplitude data for CS+ and CS– were described by Multivariate Adaptive Regression Splines (MARS; Friedman, 1991), a segmented linear regression method. The parameters of these segmented linear functions were then subjected to statistical analysis.

Given the emphasis of our study on the P1 temporal dynamics, we took the following steps to ensure that the time across subjects and conditions were comparable when we performed the above hemispheric and cross-subject averaging. First, we ensured that among the subjects included in our analyses, the trials remained after artifact rejection were approximately evenly-distributed throughout the block without leaving any major discontinuity in time (Fig. 2-2A,B). Second, since the number of remaining trials tended to vary within different experimental conditions across subjects after artifact rejection, we further equalized the number of trials prior to the 10-trial moving average by deleting trials randomly from subjects with more remaining trials. The trial deletion indexes were sampled without replacement from a uniform distribution spanning the entire block. To further ensure that deleted trials covered the block evenly,

we imposed an additional constraint such that no two consecutive trials were deleted. To demonstrate that the physical time remained comparable after the above procedure, we conducted for every condition within each subject a 10-trial moving average on the remaining within-condition trial indexes after trial equalization to estimate the approximate physical time associated with each smoothing bin used to reveal P1 temporal dynamics. We combined the hemispheric results and further performed a grand average across five subjects leaving for comparison the averaged physical time indexes between CS+ and CS–. Here we used the within-condition trial indexes (i.e., the trial order within its own presentation stream for each condition) as a proxy of the actual physical time due to the fact that all four types of trials were evenly intermixed in our experiment design. Figure 2-2C showed the averaged trial index plotted against smoothing bin index for CS+ and CS–, respectively. The close similarity between CS+ and CS– as well as the quasi-linear pattern observed for both conditions suggest that the P1 dynamics between the two conditions can be compared to assess the effect of emotional conditioning on early visual processing.

2.3 Results

2.3.1 Average ERP Analysis

The grand averaged ERPs time-locked to the onset of CS+ and CS– are shown in Figure 2-1B. A robust P1 response is seen over the parietal-occipital regions contralateral to the stimulated hemifield. Consistent with the previous report (Stolarova et al., 2006), no statistically significant difference between conditions was observed in grand averaged P1 amplitude (one-sided paired t test; left hemisphere: $p = 0.423$; right hemisphere: $p = 0.412$).

2.3.2 Single-trial Estimation of ERPs

ASEO single-trial analysis was applied to extract the ERP on a trial-by-trial basis. The process is illustrated in Figure 2-3 for a representative subject. The raw single-trial EEG time series from the right parietal-occipital area are shown in Figure 2-3A. The ASEO estimated single-trial ERPs from the data in Figure 2-3A are shown in Figure 2-3B. Ensemble averages of the data in Figure 2-3A, B are compared in Figure 2-3C. The close similarity between the two averages is taken as evidence that the ASEO method adequately estimated the single-trial ERPs and did not introduce spurious artifacts. The ongoing activities, obtained by subtracting the single-trial ERPs in Figure 2-3B from the raw single-trial data in Figure 2-3A, are shown in Figure 2-3D. The relatively constant variance of the ongoing activity for the entire epoch (mean 54.921, SD = 11) is seen as further support for the validity of the single-trial estimation procedure (Truccolo et al., 2002; Wang and Ding, 2012; Xu et al., 2009).

2.3.3 Temporal Dynamics of the P1 Component

To examine how the history of emotional conditioning affects early sensory processing, we first analyzed the temporal dynamics of the CS-evoked P1 amplitude for the conditioning block measured at sites contralateral to CS presentation across trials. The single-trial ERP data was smoothed by using a 10 trial moving average and each 10-trial ensemble was referred to a smoothing bin. Figure 2-4 demonstrates the result for a typical subject for both CS+ and CS– conditions. The P1 amplitudes, averaged across two hemispheres and across all subjects, were plotted as a function of the bin index for both CS+ and CS– in Figure 2-5. Although the amplitude of P1 elicited by CS+ is generally larger than that elicited by CS–, the difference failed to reach significance at

the level of α = 0.05, agreeing with the grand averaged ERP results reported above. However, as time progressed along the CS+ stream or the CS– stream, the temporal dynamics of the P1 amplitude revealed three distinct phases for both CS+ and CS–: (a) an initial decrease phase, (b) a subsequent increase phase, and (c) a final habituating phase.

The data in Figure 2-5A were fit by piecewise linear functions using the MARS algorithm and the result is shown in Figure 2-5B. The durations of the initial decrease phase as measured in unit of bin indexes for CS+ and CS– were both brief and covered eight and six bins, respectively. According to the relationship between smoothing bin index and trial index shown in Figure 2-2C, this decrease phase covered about 26 CS+ trials and 18 CS– trials. The slopes for CS+ and CS– conditions during this phase were –0.028 and –0.16. A t test on the slopes (Kleinbaum et al., 1988) revealed a significant condition related difference ($t(12) = 3.3174$, $p = 0.0061$) (Table 2-1). For the subsequent increase phase, the CS+ trials spanned a shorter interval (from 9 to 17 as measured by the bin index), before reaching the maximum value than the CS– trials (7 to 24). The estimated corresponding number of trials within each condition covered by this phase was 28 and 64 for CS+ and CS–. The slopes for the CS+ and CS– trials within this phase were 0.27 and 0.15. A t-test on the slopes within this phase between the two conditions revealed that the slope for CS+ trials was significantly larger than the slope for CS– trials ($t(20) = 3.1450$, $p = 0.0051$). The habituating phase for the CS+ trials covered a relatively longer period starting at about the 88th trial compared with the CS– trials which started around the 112th trial. The slopes for the CS+ and CS– trials within this phase were –0.064 and 0.0067, respectively. As characterized by the slopes within

this phase, the rate of habituation for CS+ trials was significantly larger than that for CS– trials (a slightly positive slope) ($t(64) = –8.3364$, $p < 10^{–4}$).

To demonstrate that the P1 amplitude dynamics is specific for the conditioning block, we also applied the same analysis to data from the control block and the result is shown in Figure 2-5C. In contrast to the conditioning block, no systematic changes in processing phase over trials were found during the control block. The average P1 amplitude is also significantly smaller than that of the conditioning block (one-sided t test, $p < 10^{–10}$). In addition, the relatively small variation of P1 amplitude across the entire block suggests that participants maintained a steady level of early electrocortical processing during the block. Fitting the P1 amplitude data by the MARS algorithm described above using three segments of linear functions revealed unsystematic effects between the CSs. A linear regression on P1 amplitude data across the block showed that the slopes of the linear functions were –0.0064 for CS+ and 0.0080 for CS–, respectively (Fig. 2-5D). Both slopes were considered to be close to zero.

2.4 Discussion

Emotionally salient stimuli can attract attentional resources involuntarily to affect visual processing (Müller et al., 2008). Pourtois et al. (2004), incorporating an emotional cue within a spatial orienting task, found enhanced P1 time-locked to a bar that replaced a fearful face, compared to a bar that replaced a happy face. In addition, the C1 component time-locked to the face presentation had a greater amplitude for fearful faces as compared to happy faces. In a classical conditioning paradigm, Keil et al. (2007) found gradual increase of early (60 – 90 ms) gamma band (>30 Hz) oscillations evoked by the CS+, across two consecutive experimental blocks. This was taken to

suggest that an observer's learning history would continuously alter the processing of sensory information (Moratti and Keil, 2009). In the current study, we examined this stimulus history dependent modulation in a classical delayed conditioning experiment on a more detailed time scale by means of single-trial ERP analysis (Xu et al., 2009). By extracting the P1 component evoked by the conditioning stimuli on a trial-by-trial basis, we reported three results. First, three distinct phases of P1 amplitude as a function of time specific to emotional conditioning were found: (1) a short initial decrease phase, (2) a subsequent increase phase, and (3) a final habituating phase for both the CS+ and CS– trials within the block. Second, the P1 response to CS+ stimuli exhibited slower rate of decrease over the first phase, faster rate of increase over the second phase, and again faster rate of decrease over the third phase relative to that evoked by the CS– stimuli. Third, for the control block where the same grating patterns used as CS+ and CS– stimuli in the condition block were paired with checkerboards, no systematic temporal effects were found for the P1 amplitude.

Previous work has yielded mixed results with respect to P1 differences during classical conditioning (see Stolarova et al., 2006). The present data are informative by revealing the intra-block P1 dynamics associated with learning of contingencies. One possible explanation for the initial P1 decline could be that during the early trials, the contingencies are not yet established and thus neural responses to both CSs may be subject to repetition suppression. Previous studies in human electrophysiology, neuroimaging, and primate single-cell recordings have shown that repeated stimulus presentation tends to elicit decreased neural responses over time in the visual cortex (Grill-Spector et al., 2006; Guo et al., 2007, 2008; Jiang et al., 2000, 2009; Liu et al.,

2009; McMahon and Olson, 2007). Research in classical conditioning has established that it frequently takes up to 5 trials of both the CS+ and the CS– for differential conditioning to take place, not only as reflected in psychophysiological measures, but also associated with selective enhancement in human visual cortex for the CS+ (e.g., Moratti and Keil, 2005). Considering the fact that our experiment paradigm further added a potential confounding factor by adopting a lateralized CS presenting scheme, the number of trials within the initial decrease phase (26 for CS+; 18 for CS–) might indicate the average amount of trials required to obtain conditioning effect in early visual cortex during our experiment. The smaller reduction rate for CS+ as compared to that for CS– may be reflective of the fact that any suppression was accompanied by differential enhancement for the CS+. It is worth noting that repetition suppression was not apparent in the control block, which may reflect a floor effect, given that the control block was conducted subsequent to the conditioning block, and the overall P1 amplitude was small across the control block.

After the initial decrease phase, the P1 response to both CS+ and CS– underwent a subsequent increase phase, which is consistent with an increase in the predictive value of the CSs across these trials. At this stage, increased salience for both CSs appears to lead to increased attention bias and ultimately facilitated perceptual processing in extrastriate cortex. The fact that the rate of P1 increase was greater for CS+ than for CS– suggests that the motivationally relevant predictive stimulus (i.e., the CS+) benefits more strongly from such facilitation. Hence, the difference between the slopes for CS+ and CS– during the increase phase further supports the view that

experience established during classical conditioning affects the neural network organization underlying early visual processing (Keil et al., 2007).

Functional imaging studies of visual aversive conditioning (LaBar et al., 1998; Morris et al., 1998a; Büchel and Dolan, 2000; Adolphs, 2002; LeDoux, 2003) have highlighted the amygdala, higher-order sensory areas, and frontal cortices as key structures for providing re-entrant input into visual areas (Zald, 2003; Sabatinelli et al., 2009). In addition, the amygdala has been hypothesized to mediate cortical plasticity during emotional learning (Hendler et al., 2003). Given that the visual P1 component of the ERP originates in the extrastriate cortex (DiRusso et al., 2001), and that the amygdala projects to the extrastriate cortex in primates (Amaral and Price, 1984), the differential modulatory effects of the CSs on P1 may reflect a stronger involvement of the amygdala in re-entrant sensory modulation of the CS+ as opposed to the CS–.

The final phase for both CS+ and CS– after the increase phase was a habituating phase toward the end of the conditioning block. The P1 response to the CS+ declined gradually as time progressed whereas the P1 response to CS– ceased to further increase and remained at a constant level. A widely observed activation pattern of amygdala during emotional perception and conditioning is its initial activation followed by rapid habituation or even deactivation as experiment progresses (Breiter et al., 1996; Büchel et al., 1998, 1999b; Phillips et al., 2001; Zald, 2003). Although no measurement from subcortical structures was available in our study, the habituation of the P1 amplitude across trials might reflect habituation of deep structures such as the amygdala, which may eventually cease to provide re-entry input into visual cortex.

From a network point of view, changes in connectivity as a function of learning and experience should be considered. In the domain of auditory classical conditioning, research has shown learning-induced plasticity in the receptive fields of the primary auditory areas in animals (Diamond and Weinberger, 1984; Quirk et al., 1997; Weinberger, 2004) and humans (Morris et al., 1998b). Such changes are accompanied by an increase in dopamine or acetylcholine release (Weinberger, 1995), possibly leading to long-term potentiation and the strengthening of neural connectivity (Fox and Wong, 2005). Heightened neural connectivity has been shown during viewing of emotionally salient cues (Keil et al., 2003), and directional analyses of electrocortical data in humans have suggested re-entry can be observed from higher to lower tiers of visual cortex (Keil et al., 2009). Because heightened connectivity is often associated with amplitude reduction of neural mass activity (Büchel et al., 1999b; Gruber et al., 2001), the response habituation to the CSs in our experiment might thus reflect the strengthening of visual networks representing the CSs' locations and features after repeated contingency reinforcement. This is also in line with the notion that cortical modulations during learning occur at increasingly earlier stages as learning progresses, with early trials characterized by late modulation and late trials characterized by early modulation (Stolarova et al., 2006).

Regarding the observed slope difference between the CSs, our results agree with a previous study on the impact of emotion on repetition suppression (Ishai et al., 2004). Using event-related fMRI to measure the rate of repetition suppression, Ishai et al. found that fearful faces which initially elicited stronger activation had a higher rate of repetition suppression compared with neutral faces. Although in our experiment the CSs

acquired emotional salience through conditioning, the higher P1 increase rate during the second stage coupled with subsequent stronger suppression effects for CS+ compared to CS– during the third stage suggests that processing of emotional stimuli may become more shifted toward a highly efficient neural network.

In terms of attention mechanisms during conditioning, our P1 temporal dynamics during the conditioning block support the prediction error theory of attention during conditioning (Pearce and Hall, 1980), which states that subjects' level of attention tends to decrease if a stimulus fully predicted an event during previous trials and vice versa. Studies that measured participants' attentional response via EEG and eye tracking measurements (Wills et al., 2007; Wills, 2009) have lent support to this theory by providing evidence that increased attention is correlated with prediction error. In this regard, the increase phase and the habituating phase for the CSs in our study might reflect two distinct learning stages with the increase phase indicating high uncertainty level and habituating phase indicating the opposite case according to this theory. On a neurophysiological level, these theoretical notions are consistent with the perspective that processing simple, important, and predictable information may be accomplished by increasingly early stages of visual analysis as learning progresses (Keil, 2004). Thus, initial P1 enhancement should be followed by P1 amplitude reduction (as found here), coupled with enhancement of the C1 component (60-90 ms post-stimulus). Such a pattern was observed for the CS+ when comparing blocks of an identical conditioning protocol (Stolarova et al., 2006).

In summary, by adopting a single-trial analysis method, our study revealed distinct phases of temporal dynamics of the visual P1 component within a classical emotional

conditioning paradigm. The fact that the three distinct phases of P1 amplitude dynamics were only found in the conditioning block as opposed to the control block supports the notion that the subject's emotional processing experience can constantly modulate early visual processing through conditioning. By analyzing the differential effects within each processing phase between CS+ and CS– trials we were able to examine possible neuronal mechanisms of conditioned response. Despite these positives, the present study also has limitations that should be addressed in future studies. First, owing to the stringent selection criteria (see Methods), the number of subjects is small (n = 5). Data from both hemispheres had to be combined to create a pool of sufficient trials. As a consequence, we were not able to test the hypotheses in regard to hemispheric lateralization of emotional processing (Alves et al., 2008). Second, due to the limitation of scalp-EEG, we were not able to concurrently record activities from important subcortical structures such as amygdala. Thus, the linkage between the effects observed at the cortical level and the previously established subcortical conditioning effects remains to be further substantiated. Simultaneous EEG and fMRI recording is a promising technique to overcome this weakness.

Table 2-1. Results from MARS piecewise linear regression analysis

	Segment 1 *		Segment 2 *		Segment 3 **	
	Slope	SSE	Slope	SSE	Slope	SSE
CS+	-0.0281	0.3107	0.2657	1.1858	-0.0637	3.1112
CS-	-0.1614	0.0384	0.1494	0.4713	0.0067	4.3124
Slope Difference	t-score	p-value	t-score	p-value	t-score	p-value
	3.3174	0.0061	3.1450	0.0051	-8.3364	8.24e-12

* $p < 0.01$; ** $p < 10^{-11}$

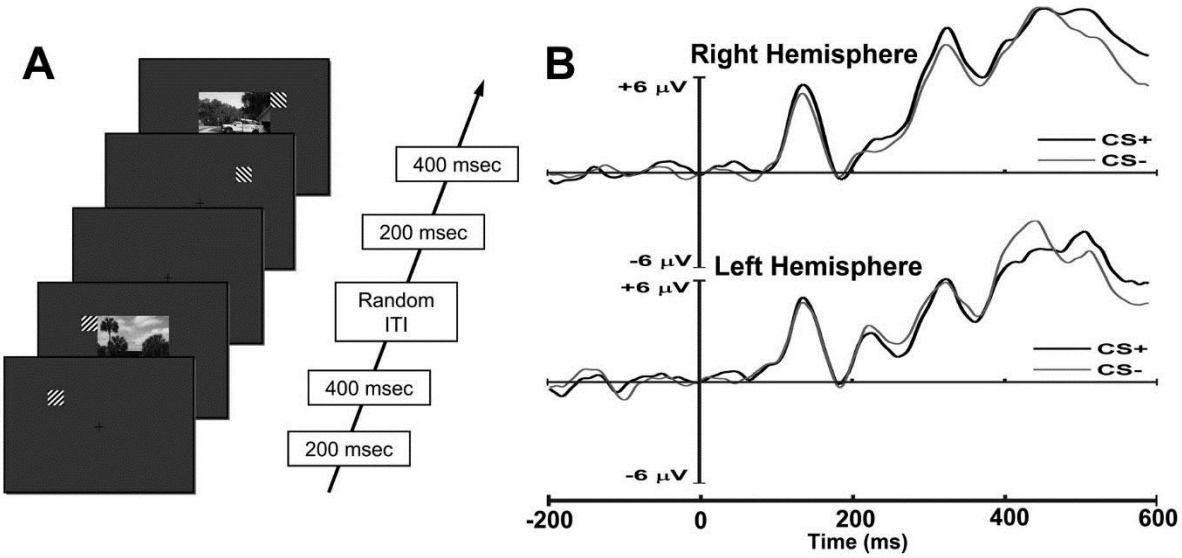

Figure 2-1. Schematic of Paradigm and ERP. A) The timeline of experiment. B) Grand average ERPs for both hemispheres and for both conditions. Condition-induced differences in P1 are not statistically significant (one-sided paired *t* test; left hemisphere: p = 0.423; right hemisphere: p = 0.412).

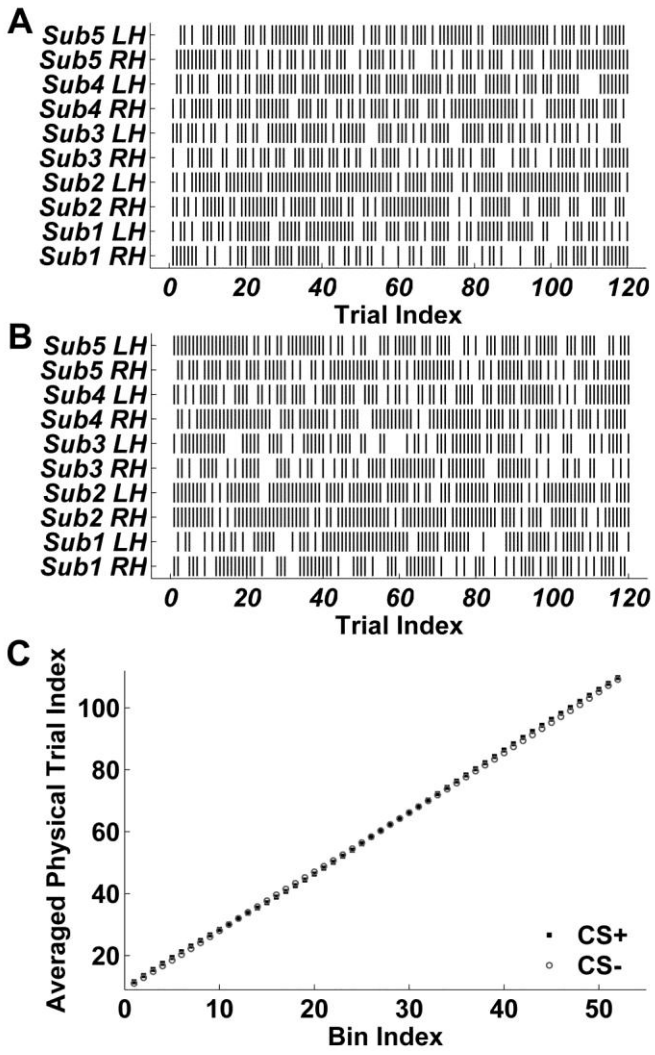

Figure 2-2. Temporal distribution of trials analyzed in this study. A) Trial raster plot for the conditioning block showing the remaining aversive (CS+) trials (vertical bars) after artifact rejection. LH: Left Hemifield and RH: Right Hemifield. The horizontal axis denotes the sequential trial index within the two experimental conditions examined in this plot: right hemifield and left hemifield CS+ trials. B) Trial raster plot showing the remaining neutral (CS–) trials for the conditioning block. C) Plot showing the relation between the smoothing bin index and the averaged within-condition trial index for the conditioning block. Note that a similar relation was observed also for the control block (not shown here).

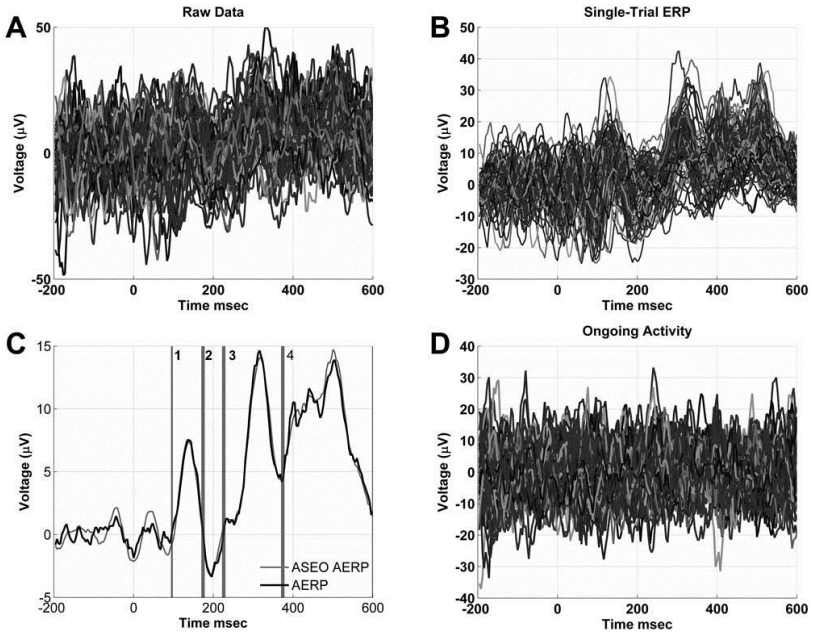

Figure 2-3. Illustration of ASEO single-trial analysis on a representative subject. A) Raw single-trial EEG data from the right parietal-occipital channel under contralateral CS+ condition. B) ASEO-estimated single-trial ERP time series. C) Average of ASEO single-trial ERPs is compared with the AERP from raw data. The four components used for initiating the ASEO algorithm were indicated. D) Single-trial ongoing activities obtained by subtracting single-trial ERPs in C) from the raw single-trial EEG data in A).

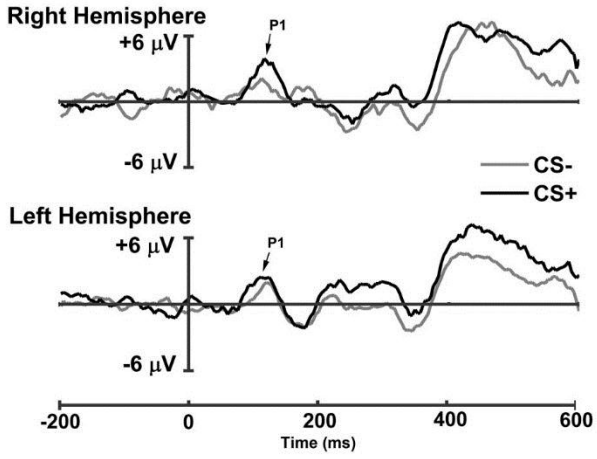

Figure 2-4. Smoothing of single-trial ERPs. Depicted are averaged single-trial ERP time series from a smoothing bin of 10 consecutive trials of the same condition. The P1 amplitude is estimated from the smoothed waveform and plotted as a function of time in Figure 2-5.

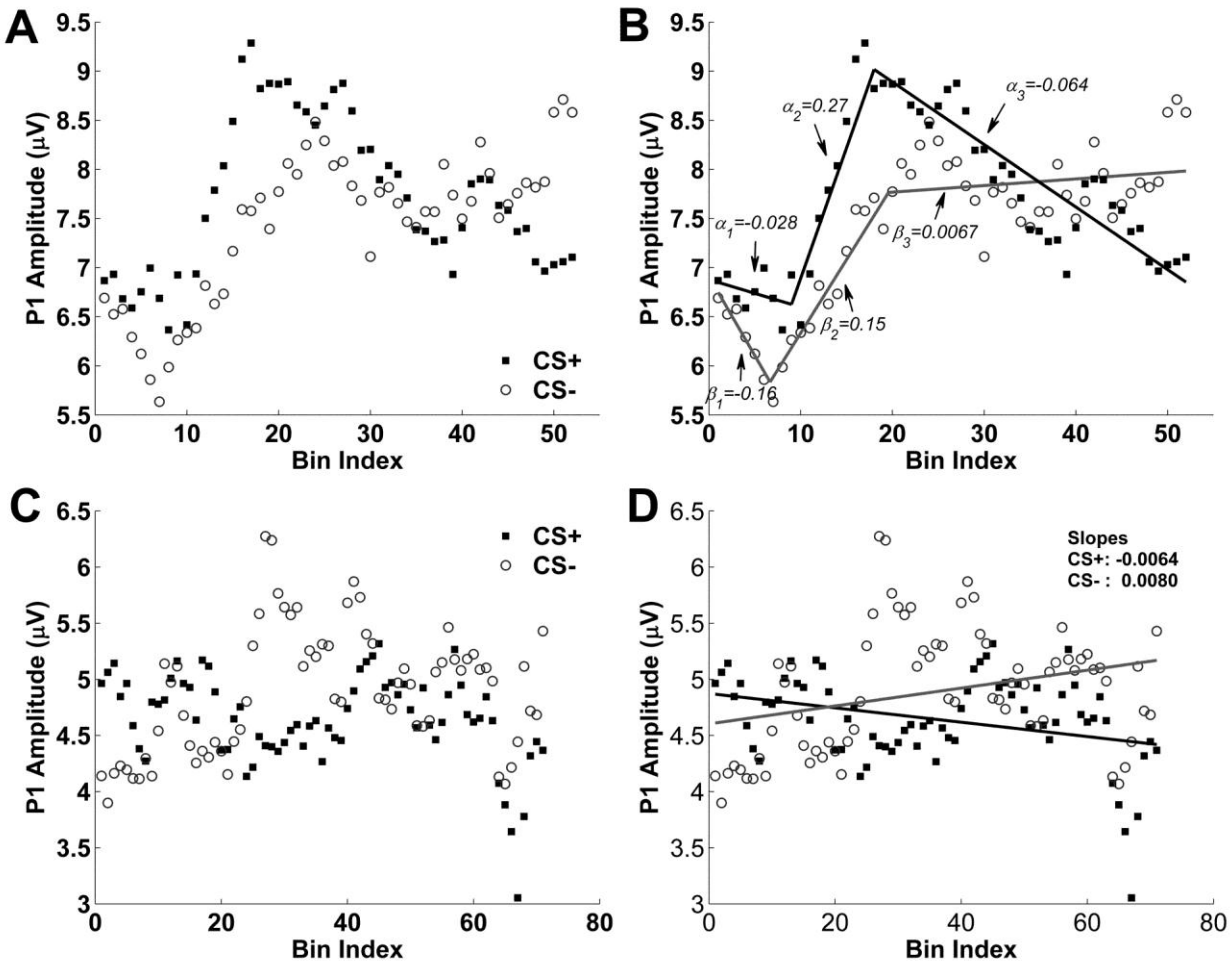

Figure 2-5. Temporal dynamics of P1 amplitude. A) The P1 amplitude as a function of smoothing bin index over the entire conditioning block for CS+ and CS−, respectively. Three distinct phases can be identified for both CS+ and CS−: an initial decrease phase, a subsequent increase phase, and a final habituating phase. B) Piecewise linear regression using MARS. *α'* s and *β'* s indicate the slopes of each segment for CS+ and CS− conditions. C) P1 amplitude sequences within the control block for CS+ and CS−. D) The linear regression analysis results for CS+ and CS− trials, respectively.

CHAPTER 3
NEURAL SUBSTRATES OF THE LATE POSITIVE POTENTIAL IN EMOTIONAL PROCESSING

3.1 Background and Significance

The event-related potential (ERP) method is used extensively in affective neuroscience. A key feature observed in ERPs evoked by emotionally engaging stimuli is the late positive potential (LPP), which is characterized by an amplitude enhancement for pleasant and unpleasant stimuli, relative to neutral stimuli, and has a centroparietal maximum topography. For affective picture viewing, LPP starts around 300 - 400 ms after picture onset, and is often sustained throughout the duration of picture presentation (Cuthbert et al., 2000). LPP amplitude has been shown to vary systematically with the experienced intensity of the affective picture content (Schupp et al., 2000; Keil et al., 2002) and exhibit abnormal patterns in mood disorders and other psychiatric conditions (Leutgeb et al., 2011; Weinberg and Hajcak, 2011; Jaworska et al., 2012). In parallel, functional magnetic resonance imaging (fMRI) have found that viewing of affective pictures is associated with increased blood-oxygen-level-dependent (BOLD) activity in widespread brain regions, including occipital, parietal, inferotemporal cortices, and amygdala (Breiter et al., 1996; Lang et al., 1998a; Bradley et al., 2003; Norris et al., 2004; Sabatinelli et al., 2005; Sabatinelli et al., 2009), suggesting that emotionally salient content enhances visual stimulus processing by attracting attentional resources (Lang et al., 1998b; Lang and Bradley, 2010). Taken together, if enhanced LPP and BOLD reflect a common underlying mechanism, one might expect a coupling between LPP amplitude and BOLD activity in the above reported regions.

A prior study recording EEG and fMRI from the same subjects but in separate sessions has found that LPP amplitude was positively correlated with BOLD responses

in lateral occipital, parietal, and inferotemporal cortices (Sabatinelli et al., 2007a). This study did not examine LPP-BOLD coupling in other higher order emotional processing areas such as prefrontal cortex and deep subcortical structures known to be involved in emotional perception (Sabatinelli et al., 2009). A more recent study using a between-subjects design observed coupling between LPP amplitude and BOLD activity in both deep and anterior structures (Sabatinelli et al., 2012), but it is still unclear whether these structures are engaged with the LPP in a category-specific way based on trial-by-trial information within each picture category. The advent of the simultaneous EEG-fMRI recording technique, together with reliable estimation of single-trial ERPs, opens new avenues to address this problem.

We recorded simultaneous EEG-fMRI while subjects passively viewed emotionally arousing and neutral pictures. The single-trial LPP amplitudes were estimated using a recently proposed method (Xu et al., 2009) and then correlated with the single-trial evoked BOLD responses across the entire brain to identify brain structures whose activity is linearly related to the trial-by-trial variation of the scalp-recorded LPP. In addition, in light of a host of prior studies reporting differential engagement of cortical and sub-cortical structures in appetitive versus aversive processing (e.g., Sabatinelli et al., 2007a), we investigated whether trial-by-trial LPP amplitude fluctuations are mediated by different neural generators during different affective states by examining the coupling between LPP amplitude and BOLD within each picture category (pleasant, neutral, unpleasant).

3.2 Methods

3.2.1 Participants

Fifteen healthy volunteers participated in the experiment in exchange of either course credits or a financial incentive of $30. One participant withdrew from the experiment. In addition, data from 3 participants were discarded due to artifacts generated by excessive movement inside the scanner. The remaining 11 participants (7 females, mean age: 20, standard deviation: 2.65) had normal or corrected-to-normal vision. The experimental protocol was approved by the Institutional Review Board of the University of Florida. Informed consent was obtained from all participants prior to the experiment.

3.2.2 Stimuli and Procedure

The stimuli consisted of 20 pleasant, 20 neutral, and 20 unpleasant pictures selected from the International Affective Picture System (IAPS, Lang et al., 2008) based on their normative valence and arousal levels. The IAPS picture numbers used in this study are: Pleasant: 4311, 4599, 4610, 4624, 4626, 4641, 4658, 4680, 4694, 4695, 2057, 2332, 2345, 8186, 8250, 2655, 4597, 4668, 4693, 8030. Neutral: 2398, 2032, 2036, 2037, 2102, 2191, 2305, 2374, 2377, 2411, 2499, 2635, 2347, 5600, 5700, 5781, 5814, 5900, 8034, 2387. Unpleasant: 1114, 1120, 1205, 1220, 1271, 1300, 1302, 1931, 3030, 3051, 3150, 6230, 6550, 9008, 9181, 9253, 9420, 9571, 3000, 3069. The selected pictures cover a wide range of contents and normative ratings. The pleasant pictures in general included sport scenes, romance, and erotic couples, whereas the unpleasant pictures incorporated threat, attack scenes, and bodily mutilations. The neutral pictures included landscapes and neutral human-beings. The mean pleasure

(valence) rating for pleasant, neutral, and unpleasant pictures was 7.0, 6.3, and 2.8, respectively. The pleasant and unpleasant pictures had similar mean arousal levels (pleasant: 5.8, unpleasant: 5.9), both being higher than neutral pictures (4.2). Pictures were chosen to be similar overall in composition, matched in jpeg size across categories, and comparable in rated complexity, to minimize confounds.

The experimental paradigm was implemented in an event-related fMRI design. Each IAPS picture was centrally displayed on a monitor for 3 seconds followed by a variable (2800 or 4300 ms) interstimulus interval (ITI). All participants completed 5 experimental sessions in which the pictures were repeated in different random orders. The order of picture presentation was also randomized across different participants. A cross was displayed at the center of the screen during the entire experiment to aid fixation. Stimuli were presented on an MR-compatible monitor using E-Prime software (Psychology Software Tools). The monitor was placed outside the scanner bore over the head of the subject. Participants viewed the task presentation in the scanner via a reflective mirror. Before the start of the first experimental session, participants were instructed to maintain eye fixation whenever the fixation cross is present and viewed the pictures without moving their eyes. After the experiment, as a validation, participants were asked to provide their ratings of 12 representative pictures (4 pictures within each category) they had not seen during the experiment along the scales of valence and arousal using a paper and pencil version of the self-assessment manikin (Bradley and Lang, 1994). The entire experiment lasted about 40 minutes.

3.2.3 Simultaneous EEG-fMRI Acquisition

MRI data were collected on a 3-T Philips Achieva scanner (Philips Medical Systems, the Netherlands). Two hundred and twelve (212) volumes of functional images were acquired using a gradient-echo echo planar imaging (EPI) sequence during each session (echo time (TE): 30 ms, repetition time (TR): 1.98 s, flip angle: 80˚, slice number: 36, field of view (FOV): 224 mm, voxel size: 3.5×3.5×3.5 mm, matrix size: 64×64). The slices were acquired in ascending order and oriented parallel to the plane connecting the anterior and posterior commissure. Slice acquisition was performed within an interval of 1850 ms during each TR, leaving an interval of 130 ms toward the end of the TR where no image acquisition was performed. This image acquisition approach allowed us to visually monitor the EEG recording within each volume during the no-scan period where EEG was not contaminated by gradient switching. A T1-weighted high resolution structural image was also obtained.

EEG data were recorded during the experiment using a 32-channel MR-compatible EEG system (Brain Products GmbH). Thirty-one sintered Ag/AgCl electrodes were placed according to the 10-20 system, and one additional electrode was placed on subject's upper back to monitor electrocardiograms (ECG). The recorded ECG will be used to detect heartbeat events to be used for the removal of the cardioballistic artifact. The EEG channels were referenced to site FCz during recording. The impedance from all scalp channels was kept below 10 kΩ during experiment as suggested by the manufacturer. EEG signal was recorded with a built-in 0.1~250 Hz band-pass filter and digitized to 16 bit at a sampling rate of 5 kHz. The digitized EEG signal was then transferred to the recording computer via a fiber-optic cable. The EEG

recording system was synchronized with the scanner's internal clock throughout the recording session to ensure the successful removal of the gradient artifact in subsequent analyses.

3.2.4 EEG Data Preprocessing

Brain Vision Analyzer 2.0 (Brain Products GmbH) was used for data preprocessing. Gradient artifacts in the EEG data were removed using a modified version of the original algorithms proposed by Allen et al. (2000). Briefly, an artifact template was created by segmenting and averaging the data according to the onset of each volume within a sliding window consisting of 41 consecutive volumes, and subtracted from the raw EEG data. To remove the cardioballistic artifact, an average artifact subtraction method (Allen et al., 1998) was used, in which R peaks were detected in the low-pass filtered ECG signal and used to construct a delayed average artifact template over 21 consecutive heartbeat events in a sliding-window approach, which was subtracted from the original EEG signal. The resulting EEG data were then low-pass filtered with the cutoff set at 50 Hz, down-sampled to 250 Hz, and re-referenced to the average reference. These data were then exported to the EEGLAB (Delorme and Makeig, 2004). SOBI (Second Order Blind Identification) (Belouchrani et al., 1993) was performed to further correct for eye-blinking, residual cardioballistic, and movement-related artifacts. Recent work has shown that SOBI is effective in removing the residual cardioballistic artifact (Vanderperren et al., 2010), as well as in separating EEG data into physiologically interpretable components (Tang et al., 2005; Klemm et al., 2009). The artifacts-corrected data were then epoched from -300 ms to 2000 ms with 0 ms being the onset of affective pictures. The prestimulus baseline was defined as -300 to 0 ms. The EEG

epochs were averaged within each condition separately to produce the average ERP (AERP). The AERP coming from each subject was further averaged across subjects to produce the grand average ERP.

3.2.5 Single-trial Estimation of LPP

Channel Pz was chosen to guide our subsequent EEG-informed fMRI analysis as it showed strong LPP difference between both emotional conditions and the neutral condition (Figure 3-1B and 3-1C). The ERP of each trial at Pz was estimated using the Analysis of Single-trial ERP and Ongoing activity (ASEO) method (Xu et al., 2009). ASEO has the following basic steps. First, according to the variable signal plus ongoing activity (VSPOA) generative model (Chen et al., 2006), the recorded EEG data for the *r*th trial ($r = 1,2,...,R$) are expressed as:

$$x_r(t) = \sum_{n=1}^{N} \beta_{rn} s_n(t - \tau_{rn}) + z_r(t) \tag{3-1}$$

where $s_n(t)$ ($n = 1,2,...,N$) is the *n* th ERP component and $z_r(t)$ is an autoregressive (AR) process modeling the ongoing activity. Within each individual trial, the n th ERP component is characterized by an amplitude scaling factor β_{rn} and a latency shift τ_{rn} to account for trial-to-trial variability. Second, using a proper initial condition, the ASEO algorithm estimates the waveforms of the ERP components and their associated amplitude scaling factors and latency shifts in an iterative fashion. Third, from scaled and latency-adjusted ERP component estimates, the single-trial ERP was reconstructed on a trial-by-trial basis. Fourth, the LPP amplitude on each trial was obtained by averaging the single-trial ERP amplitude within a time interval around the peak of LPP (see Figures 3-2 and 3-3). To date ASEO has been applied to study both monkey local

field potential data and human EEG data (Wang et al., 2008; Wang and Ding, 2011; Liu et al., 2012a, b). See Xu et al. (2009) for a more detailed description of the ASEO algorithm.

3.2.6 MRI Data Analysis

The fMRI data were processed using SPM5 (http://www.fil.ion.ucl.ac.uk/spm/). The first five volumes in an experimental session were discarded to allow the scanner to stabilize. Slice timing was corrected using sinc interpolation to account for differences in acquisition time. The images were then corrected for head movement by spatially realigning the images to the sixth image of each session. Images were further normalized and registered to a standard template within SPM (the Montreal Neurological Institute (MNI) space). The functional volume images were resampled to a spatial resolution of 3×3×3 mm. The transformed images were then smoothed by a Gaussian filter with a full-width at half-maximum (FWHM) of 8 mm. The low frequency temporal drifts were removed from the functional images by applying a high-pass filter with a cut-off frequency of 1/128 Hz, and the global signal was removed by dividing every voxel in a slice by the estimated global signal value.

Two separate general linear models (GLMs) with parametric modulation were constructed to model the relationship between LPP amplitude and BOLD. In the first model, we were mainly interested in examining the overall LPP-BOLD coupling across all three picture categories (i.e. pleasant, neutral, and unpleasant). Therefore, in this model we combined all three picture categories and modeled the resulting single experimental condition with two task-related regressors. The first regressor described the combined condition and consisted of a sequence of boxcar functions with unit height

synchronized with the onset of pictures. The width of each boxcar function was set to the duration of picture presentation (3 s). For the second regressor, the height of the boxcar functions in the first regressor varied according to the ASEO-estimated single-trial LPP amplitude, with the mean level of the single-trial LPP amplitudes removed (Figure 3-3C). This regressor was intended to account for both the between-category and the within-category variability in LPP amplitude and its correlation with BOLD. The two regressors were further convolved with a canonical hemodynamic response function (HRF) before being incorporated into the design matrix. Six regressors describing the subjects' head movement obtained from image preprocessing were further introduced to account for any movement related artifacts during scan. We referred to our first model as the "full model." A single contrast was performed based on this model resulting in one statistical map for each subject.

In the second model, we included six task-related regressors, with three corresponding to the three picture categories (pleasant, neutral, and unpleasant), and the other three modeling the relationship between LPP amplitudes and BOLD within each picture category. Since this model captures trial-by-trial coupling between LPP amplitude and BOLD within each picture category, we refer to it as the "within-category model". The three regressors modeling the three picture categories consisted of sequences of boxcar functions with unit height placed according to the picture onset within the corresponding categories. The width of the boxcar functions remained the same as those in the "full model" (3 s). For regressors modeling trial-by-trial LPP-BOLD coupling, we further scaled the height of the boxcar functions with the corresponding mean removed single-trial LPP amplitudes within each picture category. Similar to the

full model described above, the six task-related regressors were convolved with a canonical HRF. Additional six regressors describing subjects' head movement were also introduced as covariates in the model. The following contrasts were performed based on this model: pleasant vs. neutral, unpleasant vs. neutral, LPP-BOLD coupling within each category (pleasant, neutral, and unpleasant).

Second-level analyses was performed using random effects models based on the statistical maps obtained from the within-subjects analyses to examine reproducible effects across all subjects. For conventional BOLD contrasts, the group level T-maps were thresholded at $p < 0.05$ (FDR corrected). For LPP-BOLD coupling, because it is derived from the trial to trial variability signal on top of the large picture-evoked response, and this residual variability is generally smaller than the large picture-evoked response and may contain other ongoing brain processes that are not related to the experimental task, the correlation was generally smaller and required a more relaxed statistical threshold. In line with recent studies using EEG-informed fMRI analysis (see, e.g., Debener et al., 2005; Eichele et al., 2005; Bénar et al., 2007; Scheeringa et al., 2011), for LPP-BOLD coupling effects, the group level T-maps were thresholded at $p < 0.003$ (uncorrected). A cluster-level threshold of $k = 5$ voxels was further imposed.

3.3 Results

3.3.1 ERP Analysis

Post-experiment ratings of 12 representative pictures indicate that the subjects correctly distinguished the three categories of pictures (valence: pleasant = 6.5; neutral = 5.3; unpleasant = 2.6; arousal: pleasant = 4.7; neutral = 2.9; unpleasant = 4.0). Figure 3-1A shows enhanced positivity for both pleasant and unpleasant pictures, relative to

neutral pictures, in the grand average ERP at Pz, starting from about 300 ms after picture onset. Since the time interval during which LPP reached a maximum was relatively broad, the LPP amplitude was measured by taking the mean within 300 to 600 ms. A one-way analysis of variance on LPP amplitudes with repeated measures identified a significant picture category-related difference in LPP amplitudes ($F(2,20) = 23.11$, $p < 0.05$). As further indicated by the results of post-hoc tests with Bonferroni adjusted significance level, the mean LPP amplitudes for both the pleasant ($M = 3.153$, $SD = 1.733$) and unpleasant ($M = 3.090$, $SD = 2.048$) pictures were significantly larger than that for the neutral pictures ($M = 1.523$, $SD = 1.684$; pleasant vs. neutral: $t(10) = 6.26$, $p < 0.001$; unpleasant vs. neutral: $t(10) = 5.65$, $p < 0.001$). However, no significant difference was found in LPP amplitudes between the pleasant and unpleasant categories ($t(10) = 0.227$, $p = 0.825$). The ERP difference topography further confirmed that the positivity is strongest among parietal channels for both pleasant and unpleasant conditions (Figure 3-1B and 3-1C), agreeing with prior ERP studies of emotion and motivation (e.g. Lang and Bradley, 2010). The enhanced positivity was sustained throughout the duration of picture presentation for both pleasant and unpleasant pictures.

Artifact-removed raw EEG data and ASEO-estimated single-trial ERPs at Pz are shown in Figure 3-2A and 2B for a representative subject. Displayed as raster plots in Figure 3-2C and Figure 3-2D, the ASEO-estimated single-trial ERPs improved signal-to-noise ratio, and preserved the trial-by-trial dynamics of the LPP amplitude, which is important because the single-trial LPP amplitudes were used to correlate with BOLD response in subsequent analyses. The validity of the single-trial ERPs can be further

supported by averaging the data in Figure 3-2A and 3-2B (Xu et al., 2009; Wang et al., 2008; Wang and Ding, 2011). The similarity between ASEO AERP and the original AERP indicated that the algorithm accurately estimated the single-trial ERPs from the raw data (Figure 3-2E). Figure 3-3A and 3-3B display single-trial LPP amplitudes as functions of trial index. From these two figures, one can see that, on average, the single-trial LPP amplitudes for both pleasant and unpleasant pictures are higher than those for the neutral condition, yielding further support for the grand average ERP result in Figure 3-1. The estimated single-trial LPP amplitudes were used to scale the boxcar functions to examine the relationship between LPP amplitude and BOLD (Figure 3-3C).

3.3.2 fMRI Analysis

The traditional fMRI group level activation maps contrasting 1) pleasant against neutral and 2) unpleasant against neutral picture categories are shown in Figure 3-4A and 3-4B. Both pleasant and unpleasant pictures activated the emotion-processing network, encompassing the visual cortices and deep structures. Specifically, relative to neutral pictures, pleasant pictures mainly activated areas in bilateral occipito-temporal junctions, bilateral posterior parietal cortices, medial prefrontal cortex, and left orbital frontal cortex. Other activated areas included fusiform gyrus, lingual gyrus, middle frontal gyrus, supramarginal gyrus, parahippocampal gyrus, and temporal pole (Figure 3-4A). Unpleasant pictures mainly activated areas such as the bilateral occipito-temporal junctions, bilateral posterior parietal cortices, bilateral ventral lateral prefrontal cortices, left orbital frontal cortex, bilateral amygdalae/hippocampi, insula, and supplementary motor area. Other activated areas included fusiform gyrus, lingual gyrus, supramarginal gyrus, temporal pole, and postcentral cortex (Figure 3-4B). In general,

the activation results agree with a previous report employing a similar experimental protocol (Sabatinelli et al., 2007a), and serve to demonstrate that the quality of the fMRI data is preserved despite the presence of the EEG recording system in the scanner.

3.3.3 Trial-by-trial Coupling of LPP and BOLD

To assess the coupling between the LPP amplitude and BOLD, the coefficients for regressors associated with LPP amplitude variations were examined. Using the "full" model, which combined the neutral, pleasant, and unpleasant picture categories as a single regressor to describe the effect of both between- and within-category LPP amplitude variations on BOLD, the single-trial LPP amplitude was positively correlated with evoked BOLD responses in bilateral occipito-temporal junctions, insula, amygdala/hippocampus, temporal poles, and left orbital frontal cortex (Figure 3-5A).

Using the "within-category" model, which allowed us to examine the coupling between LPP and BOLD within each picture category, it was found that for the neutral condition, no significant coupling between single-trial LPP amplitude and BOLD existed among subjects. For the pleasant condition, the single-trial LPP amplitude was positively correlated with BOLD responses in bilateral occipito-temporal junctions, amygdala, temporal poles, precuneus, right nucleus accumbens (NAcc), medial prefrontal cortex (MPFC), and cerebellum (Figure 3-5B). For the unpleasant condition, the single-trial LPP amplitude was positively correlated with BOLD responses in bilateral ventral lateral prefrontal cortices, bilateral insula, temporal poles, precuneus, left middle temporal cortex, and left postcentral cortex (Figure 3-5C). Table 3-1 listed the MNI coordinates of these regions. It is worth noting that we did not find any structures in

which BOLD was negatively correlated with LPP amplitude under the same significance level.

3.4 Discussion

Emotional stimuli evoke a late positive potential (LPP) which is interpreted to signify enhanced attention and visual processing (Bradley, 2009). This signature ERP response is known to be altered in mood disorders and other related psychiatric illnesses (Foti et al., 2010; Leutgeb et al., 2011; Weinberg and Hajcak, 2011; Jaworska et al., 2012; Weymar et al., 2012). Despite the importance of LPP its neural substrate is not clear. ERP source localization is only partly successful (Keil et al., 2002; Sabatinelli et al., 2007a). This problem is addressed here by recording simultaneous EEG and fMRI while subjects viewed IAPS affective pictures. Extracting LPP on a trial-by-trial basis, the overall LPP amplitude variability across three picture categories (pleasant, neutral and unpleasant) was found to be correlated with BOLD responses in an extensive cortical and subcortical network, including visual cortices and deep emotion-processing structures. In addition, consistent with the notion that appetitive and aversive information may engage different neural substrates, the brain areas where BOLD activity was correlated with LPP amplitude during pleasant picture viewing were not the same as those during unpleasant picture viewing.

3.4.1 Methodological Considerations

Prior investigation of the association between LPP and evoked BOLD responses relied on recording EEG and fMRI over separate sessions and correlating averaged responses across subjects (Sabatinelli et al., 2007a; Sabatinelli et al., 2012). One potential drawback of such an approach is that it is difficult to keep the psychological

and biological conditions exactly the same in different recording sessions, and moreover, the correlation between average LPP and BOLD does not reflect their trial-by-trial co-variations and coupling towards individual pictures within each subject. A new technology, simultaneous EEG-fMRI, has become available over the past few years. As has been recently demonstrated (Nagai et al., 2004; Eichele et al., 2005; Debener et al., 2005; Scheeringa et al., 2011), simultaneous EEG-fMRI is capable of overcoming these limitations, and has the potential to allow the interrogation of trial-by-trial associations between the two recording modalities. The present study benefits from another methodological development. Applying a recently proposed single-trial analysis algorithm called ASEO we were able to estimate the LPP amplitude on a trial-by-trial basis. The improved signal-to-noise ratio helps to more fully reveal the brain areas whose BOLD responses are correlated with LPP fluctuations. The ASEO algorithm has been tested in both monkey local field potential data (Wang et al., 2008; Xu et al., 2009) and human scalp EEG data (Fogelson et al., 2008; Wang and Ding, 2011; Liu et al., 2012a, b), and proven useful to address questions arising in a number of contexts, ranging from the proper preprocessing of event-related data for functional connectivity analysis to the temporal dynamics of emotional conditioning.

3.4.2 LPP-BOLD Coupling and Its Theoretical Significance

The brain regions where BOLD activities co-vary with single-trial LPP amplitude across three picture categories reflected a joint involvement of the visual system and a network of structures known to be associated with emotional processing. Past source-space modeling of LPP has only been able to identify generators in the visual system, including occipito-temporal, parietal, and inferior temporal cortices (Keil et al., 2002;

Sabatinelli et al., 2007a), despite the fact that the amplitude of LPP is closely related to the rated intensity of emotion (Schupp et al., 2000; Keil et al., 2002). In line with a recent study (Sabatinelli et al., 2012), the present study extends the prior findings by showing that deep structures such as the insula and the amygdala, along with visual structures, contribute to the generation of LPP and its amplitude modulation. These results provide further evidence supporting the view that emotional pictures naturally attract attentional resources as a result of the engagement of the fundamental motivational system (Cacioppo et al., 1993, 1994; Palomba et al., 1997; Lang et al., 1997, 1998b; Schupp et al., 2000; Pastor et al., 2008; Lang and Bradley, 2010).

The contribution to scalp-recorded potentials by the emotional processing areas may be modulatory and mediated by the visual cortex. It has been hypothesized that when observers view emotionally engaging scenes cortical and deep subcortical structures modulate visual cortex in a re-entrant fashion (Keil et al., 2009; Pessoa and Adolphs, 2010). These structures include the amygdala, insula, and prefrontal cortex (Rotshtein et al., 2001; Phan et al., 2002; Adolphs, 2002; LeDoux, 2003; Zald, 2003; Luo et al., 2007). As evidenced by recent human intracranial studies, amygdala and orbitofrontal cortex show fast responses to the emotional content of stimuli, which would enable them to provide re-entrant feedback to the visual cortices (Oya et al., 2002; Krolak-Salmon et al., 2004), to potentially affect the gain of visual neurons. In addition, the activation of emotion-related BOLD modulations in the amygdala is found to precede that in the fusiform gyrus, the medial occipital gyrus, and the calcarine fissure, consistent with the amygdala's putative role in initiating the re-entrant interaction (Sabatinelli et al., 2009). Taken together, the positive correlation found in the current

study between single-trial LPP amplitude and BOLD activity in the amygdala, insula and areas in prefrontal cortex is supportive of the re-entrant hypothesis of emotional perception.

3.4.3 Category-specific Network Processing

Restricting to pictures within each valence category revealed category-dependent differences in regions showing LPP and BOLD coupling. For pleasant pictures, LPP amplitude variability was found to be linearly related to BOLD activity in bilateral amygdalae, whereas for unpleasant pictures, this correlation was absent. This finding was further corroborated by a contrast of LPP-BOLD coupling maps between pleasant and unpleasant conditions showing that the amygdala was preferentially engaged in LPP modulation in the pleasant condition. For the unpleasant pictures, the amygdala was found to be activated by a traditional fMRI contrast between unpleasant and neutral conditions, suggesting a rather constant level of amygdala activation on a trial-by-trial basis. Specifically, while the amygdala activity is clearly enhanced by unpleasant pictures as a whole, it does not co-vary with trial-by-trial LPP changes for different pictures within this category. This may reflect a limited response variability of the amygdala for unpleasant scenes or the presence of additional sources of variance that govern the modulation of LPP. A wider selection of unpleasant scenes may help to identify the potential sources of co-variation between electrophysiological measures and amygdala BOLD activity during aversive/defensive engagement.

Whether amygdala responds to pleasant stimuli is debated, although several studies reported amygdala activation during processing of pleasant stimuli, especially when these stimuli have highly arousing erotica content (Lane et al., 1997; O'Doherty et

al., 2001; Hamann et al., 2002; Zald, 2003). In the present study, the fact that the amygdala was not activated in a traditional fMRI analysis by contrasting the pleasant with the neutral category may indicate that the overall mean amygdala BOLD response to pleasant pictures was small. Yet, the positive correlation between LPP amplitude and BOLD activities in bilateral amygdalae suggests that the BOLD fluctuations in the amygdala is parametrically related to intensity variations of pleasant emotional content, as measured by the LPP. This finding further demonstrates that combining electrophysiological recordings and functional imaging can yield information not possible with either modality alone.

The LPP-BOLD coupling was found in MPFC and NAcc only for pleasant pictures. Contrasting LPP-BOLD coupling maps between pleasant and unpleasant conditions showed that the MPFC is preferentially coupled with LPP in the pleasant condition. In addition, the MPFC was activated by contrasting pleasant with neutral pictures, but the same region was not activated when comparing unpleasant and neutral pictures. NAcc and MPFC are densely interconnected (Ferry et al., 2000; Roberts et al., 2007) and often show correlated activities in human reward studies (Knutson et al., 2003; Rogers et al., 2004), leading to the view that both NAcc and MPFC are part of the human reward system mediating appetitive behaviors. Several studies have reported involvement of both structures in the perception of pleasant emotional stimuli including attractive faces, romance, and erotica (Aharon et al., 2001; Karama et al., 2002; O'Doherty et al., 2003; David et al., 2005; Ferretti et al., 2005; Sabatinelli et al. 2007b) as well as in vivid imagery of pleasant scenes (Costa et al., 2010). Hence, the observed

positive correlation between LPP amplitude and key structures in the reward system may reflect the contribution to the cortical potential by the appetitive system.

For unpleasant pictures, the LPP was correlated with BOLD in insula and adjacent temporal and ventrolateral prefrontal cortices (VLPFC). The same regions were found to be active when contrasting unpleasant with neutral pictures. It has been shown repeatedly that the human insula is involved in tasks that challenge the representation of bodily states as well as processing of emotions (Craig, 2009; Gu et al., 2010; Fan et al., 2011), especially for aversive emotions such as disgust and threat (Phillips et al., 1997, 1998; Adolphs, 2002; Straube and Miltner, 2011). Reliable co-variation of the insula and peri-insula with the LPP during aversive perception demonstrates that these structures contribute to the modulation of cortical potential during aversive events. It also suggests that the aversive/defensive circuitry involved in processing unpleasant pictures is not engaged in an all-or-none fashion, but varies parametrically as a function of aversive motivation, indexed by the LPP amplitude. It is worth noting that insula was not activated when LPP-BOLD coupling maps were contrasted between pleasant and unpleasant conditions. In light of the finding that insula is activated during viewing of highly arousing pleasant stimuli (e.g. erotica; Karama et al., 2002), this may suggest that for pleasant pictures, insula is engaged in LPP modulation but the degree of modulation did not reach the level of statistical significance.

Finally, for both pleasant and unpleasant pictures, BOLD activity in regions within midline parietal cortex is linearly correlated with the LPP. For pleasant pictures, the region that was most correlated with LPP amplitude was within the precuneus, whereas for unpleasant pictures, such correlation occurred in more ventral regions, particularly

the posterior cingulate cortex and precuneus. The involvement of these parietal regions is in line with electrophysiological data and with the theoretical notion of “motivated attention” in which features of emotionally arousing scenes attract perceptual processing resources (Keil et al., 2002; Keil et al., in press).

Table 3-1. Regions showing coupling between LPP amplitude and BOLD

Anatomical Regions	Side	MNI Coordinates (x,y,z)	Z-score
Three picture categories combined:			
Occipital Cortex	Left	-27, -96, 3	3.33
	Right	27, -99, 15	3.62
Superior Temporal Cortex	Left	-45, -3, -6	3.51
	Right	45, 0, -9	3.19
Middle Temporal Cortex	Left	-45, -63, -3	3.00
Inferior Temporal Cortex	Right	54, -63, -12	3.18
Insula	Left	-45, 9, -9	4.30
	Right	42, -6, -6	3.83
Orbitofrontal Cortex	Left	-30, 12, -15	3.33
Amygdala/Hippocampus	Left	-24, -3, -24	3.07
	Right	21, -6, -19	3.18
Temporal Pole	Left	-33, -3, -42	3.10
	Right	27, -3, -42	3.62
Pleasant pictures:			
Occipital Cortex	Left	-33, -90, -9	3.83
	Right	33, -87, -6	4.81
Middle Temporal Cortex	Left	-53, -72, 12	3.63
	Right	60, -60, 9	4.49
Inferior Temporal Cortex	Right	54, 63, -6	3.41
Amygdala	Left	-21, 0, -18	4.28
	Right	21, 0, -18	3.67
Temporal Pole	Left	-27, 6, -21	3.94
	Right	42, 21, -27	4.27
Precuneus		3, -48, 57	3.75
Medial Prefrontal Cortex	Right	9, 63, 15	3.47
Cerebellum	Left	-45, -63, -24	3.63
Nucleus Accumbens	Right	6,12,-9	3.36
Unpleasant pictures:			
Ventral Lateral Prefrontal Cortex	Left	-51, 33, 0	4.19
	Right	57, 33, 6	3.20
Middle Temporal Cortex	Right	51, -6, -15	3.60
Temporal Pole	Left	-57, 0, -6	3.20
	Right	54, 9, -9	3.63
Insula	Left	-39, 9, -3	3.05
	Right	45, 12, -6	3.39
Precuneus	Left	-12, -51, 21	3.34
Postcentral Cortex	Left	-27, -36, 57	3.18

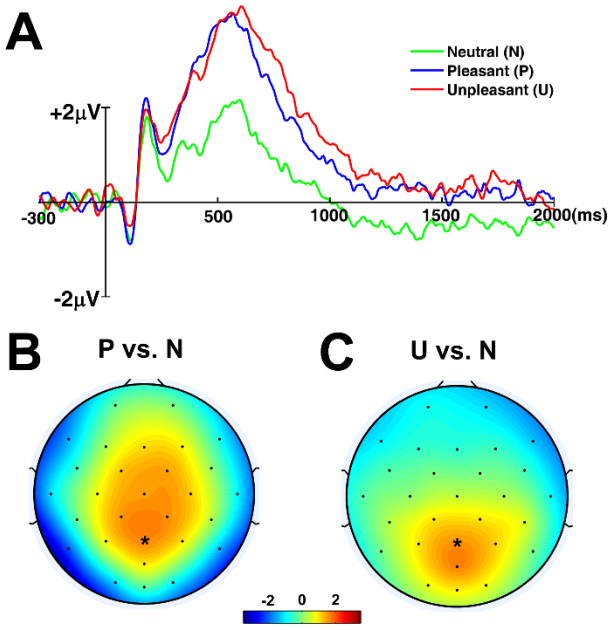

Figure 3-1. ERP analysis. A) Grand average (n = 11 subjects) ERP showing the LPP at Pz with time zero set to the onset of pictures. B) The scalp topography showing the ERP difference between pleasant and neutral conditions. Here ERP was averaged within the time interval from 300 to 600 ms. C) The scalp topography showing the ERP difference between unpleasant and neutral conditions. Here ERP was averaged within the same interval.

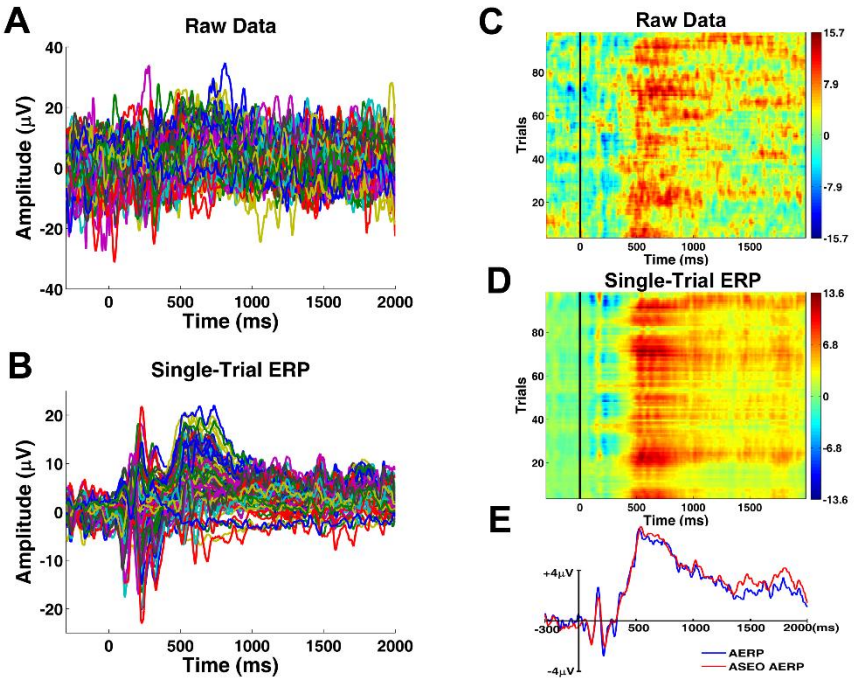

Figure 3-2. Single-trial ERP analysis. A) Epoched EEG data at Pz from a representative subject after artifact removal. B) Single-trial ERPs estimated using ASEO from data shown in A. C) Raster plot of the EEG data in A (smoothed with a moving average across 5 trials for visualization purpose). D) Raster plot of single-trial ERP data in B smoothed the same way as in C. E) Comparison between averaged ERP (AERP) using data in A and averaged ASEO single-trial ERPs (ASEO AERP) using data in B.

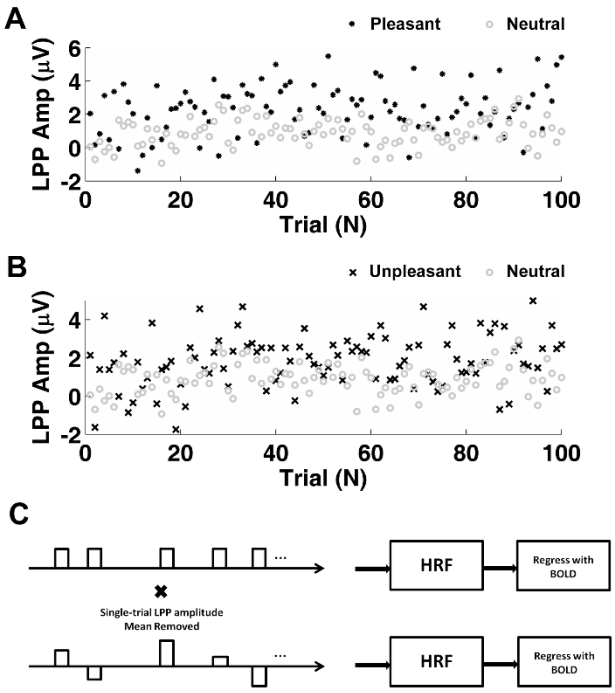

Figure 3-3. Single-trial LPP dynamics. A) Trial-by-trial LPP amplitude for the pleasant and neutral conditions. B) Trial-by-trial LPP amplitude for the unpleasant and neutral conditions. The horizontal axes in A and B represent the sequential index of picture presentation within each picture category. C) Schematic illustrating the use of single-trial LPP amplitude as a parametric modulation in GLM. The height of each boxcar function is scaled by the mean-removed LPP amplitude.

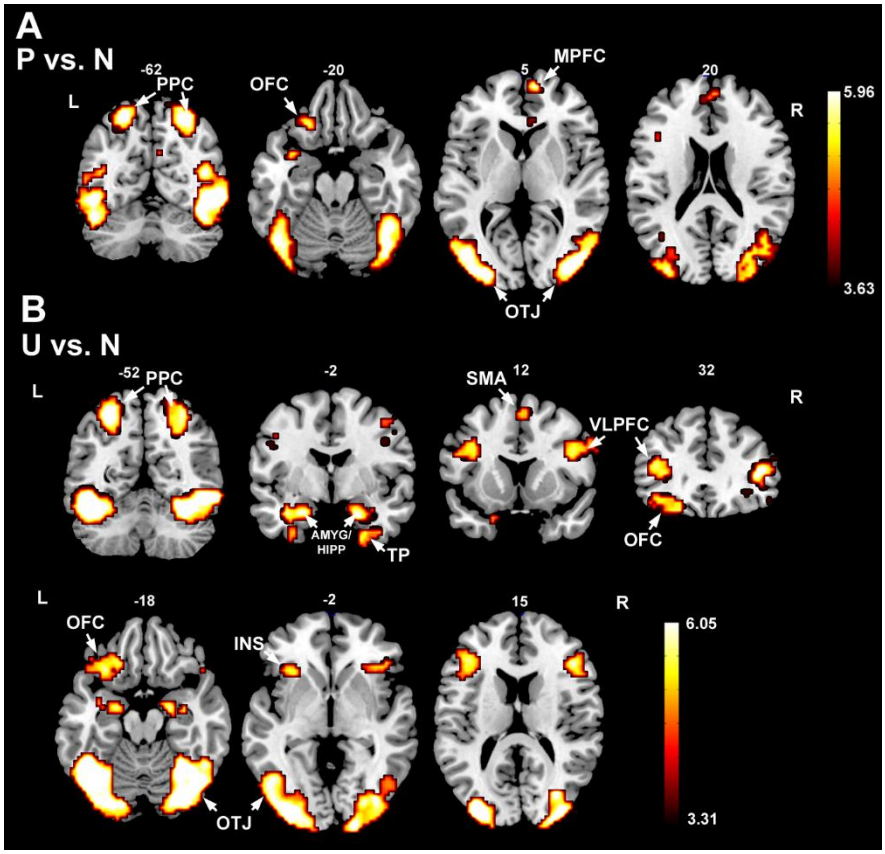

Figure 3-4. Activation maps based on BOLD contrast. A) Pleasant vs. Neutral (P vs. N) condition. B) Unpleasant vs. Neutral (U vs. N) condition. Activations are thresholded at p = 0.05 FDR corrected. PPC: posterior parietal cortex, OFC: orbital frontal cortex, MPFC: medial prefrontal cortex, OTJ: occipitotemporal junction, AMYG: amygdala, HIPP: hippocampus, TP: temporal pole, SMA: supplementary motor area, VLPFC: ventral lateral prefrontal cortex, INS: insula.

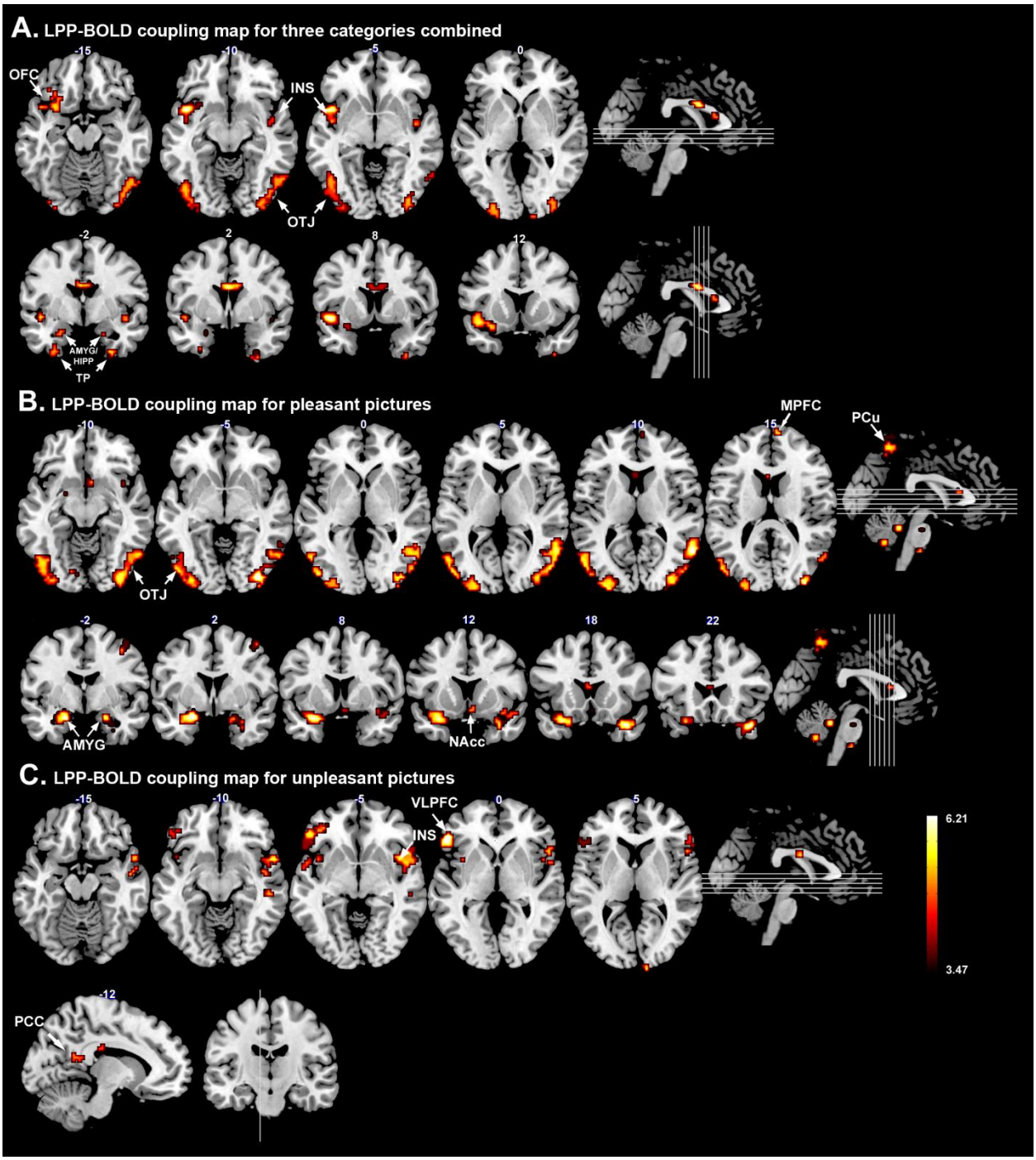

Figure 3-5. LPP-BOLD coupling maps where highlighted regions indicate significant correlation between trial-by-trial fMRI response and the corresponding single-trial LPP amplitude. A) Pleasant, Neutral, and Unpleasant combined. B) Pleasant. C) Unpleasant. All maps are thresholded at p = 0.003. A cluster threshold k = 5 is further applied. OTJ: occipitotemporal junction, INS: insula, AMYG: amygdala, HIPP: hippocampus, TP: temporal pole, PCu: precuneus, PCC: posterior cingulate cortex, MPFC: medial prefrontal cortex, VLPFC: ventrolateral prefrontal cortex, NAcc: nucleus accumbens.

CHAPTER 4
MODULATION OF ALPHA OSCILLATIONS IN ANTICIPATORY VISUAL ATTENTION: CONTROL STRUCTURES REVEALED BY SIMULTANEOUS FMRI-EEG

4.1 Background and Significance

Our ability to focus attention is a core cognitive faculty. Uncovering the neuronal mechanisms of attention remains a key challenge for neuroscience and represents an essential goal in the translational efforts to mitigate attention deficits in a variety of psychiatric and neurological disorders. Extensive research on selective attention has focused on stimulus-evoked responses and their attentional modulation. It is becoming increasingly clear that a complete understanding of attention mechanisms requires improved knowledge of the processes that underlie the deployment and control of attention in advance of sensory stimulation. In particular, how higher-order brain areas control sensory cortices to prospectively enhance the processing of behaviorally relevant signals and suppress the processing of behaviorally irrelevant distractors remains largely unknown.

The modulation of posterior alpha oscillation (8 – 12 Hz) following an attentional cue is a robust neural marker signifying selective sensory biasing by covert attention via top-down mechanisms. When covert attention is directed to one side of the visual field, alpha oscillation is more strongly suppressed over the hemisphere contralateral to the attended hemifield (Worden et al., 2000; Sauseng et al., 2005; Thut et al., 2006; Rajagovindan and Ding, 2011). Such desynchronization and hemispheric lateralization of alpha are thought to reflect an increase in cortical excitability among task-relevant sensory cortices to facilitate upcoming input processing (Sauseng et al., 2005; Thut et al., 2006; Romei et al., 2008). Putative sources of the top-down control signals include the dorsal frontoparietal attention network and other higher-level executive regions

known to mediate goal-directed behaviors (Kastner et al., 1999; Shulman et al., 1999; Corbetta et al., 2000; Hopfinger et al., 2000; Corbetta and Shulman, 2002; Astafiev et al., 2003; Giesbrecht et al., 2003). Two recent studies employing repetitive transcranial magnetic stimulation (rTMS) showed disrupted alpha lateralization after selectively disturbing the activities in FEF and IPS (Capotosto et al., 2009, 2012), providing evidence of top-down modulation of alpha by the dorsal attention network. Evidence from non-perturbative testing, however, has remained scarce.

The simultaneous EEG-fMRI technique opens avenues to address this problem. Resting-state studies have established the feasibility of the technique by revealing correlations between alpha amplitude and blood-oxygen-level-dependent (BOLD) activities in both the frontoparietal and default mode networks (Laufs et al., 2003a, 2003b, 2006; Moosmann et al., 2003; Mo et al., 2013). In the present study we recorded simultaneous EEG-fMRI from subjects performing a cued spatial visual attention task. Correlating single-trial alpha power and alpha lateralization with BOLD activity across the entire brain, we wish to identify sources responsible for different aspects of alpha attentional modulation. Besides the dorsal attention network, we further hypothesized that the “core system” is also involved in top-down attentional modulation, in light of the latter’s function in mediating goal-directed behaviors (Dosenbach et al., 2006, 2007, 2008).

4.2 Materials and Methods

4.2.1 Participants

The experimental protocol was approved by the Institutional Review Board at the University of Florida. Eighteen right-handed college students with normal or corrected-

to-normal vision and no history of mental disorders gave written informed consent and participated in the study in exchange for course credits. Data from five participants were excluded due to one of the following three reasons: 1) poor behavioral performance (1 participant), 2) difficulties in following task instructions (1 participant), and 3) excessive body or eye movement (3 participants). The remaining thirteen participants (5 females) have a mean age of 19 (SD = 1.34).

4.2.2 Paradigm

Stimuli were displayed on a 30-inch MR-compatible LCD monitor with 60 Hz refresh rate which was placed outside of the scanner bore over the head of the subject. Participants viewed the stimulus presentation via a reflective mirror system with a viewing distance of approximately 230 cm. Within an experimental session, participants were instructed to maintain constant fixation on a white point positioned at the center of a gray background. Two additional points were placed at the lower left and lower right peripheral visual fields (5˚ lateral to the central fixation and 1.2˚ below the horizontal meridian) to mark the locations where target stimuli would appear.

As illustrated in Figure 4-1, in the paradigm, each trial began with a cue presented slightly above the central fixation point briefly for 200 ms, which instructed the participant to covertly direct their attention to either the lower left or lower right visual field. Left-directing cue and right-directing cue has equal probability. Following a variable cue-target interval randomized between 2000 and 8000 ms, target stimuli comprised of vertical black-and-white gratings (100% contrast; 1.7˚ in viewing angle) were flashed briefly for 100 ms at one of the marked peripheral spatial locations with equal probability (50% target validity). When target stimuli appeared at the attended

spatial location, participants were required to discriminate the spatial frequency (5.5 vs. 5.0 cycles per degree) of the gratings and make a speedy 2-button choice using their right index or middle fingers without sacrificing accuracy. Stimuli occurred at the unattended location were ignored. The inter-trial interval (ITI) was randomized between 2000 ~ 8000 ms. In addition to the two instructional cues (left or right), there was a third type of cue in the experiment which instructed the participants to freely select the visual field to attend. The data from the choice cue were not analyzed here. The symmetric symbols used as cues, T, O and ◊, were counterbalanced across subjects.

All participants went through a training session before the actual experiment to ensure that proper eye fixation as well as a reasonable level of performance could be maintained (above 70%). The task was divided into multiple sessions with the length of each session kept around six minutes to help participants maintain a constant level of attention within the session. The participants completed between eight and twelve sessions for the experiment. A short break was administered between two adjacent sessions.

4.2.3 EEG Data Acquisition and Preprocessing

Continuous EEG data was collected during the experiment with a 32-channel MR-compatible EEG recording system (Brain Products). Thirty-one sintered Ag/AgCl electrodes were placed on the scalp according to the 10-20 system. One additional electrode was placed on the subject's upper back to record electrocardiogram (ECG), which was subsequently used to remove the cardioballistic artifact during EEG preprocessing. The impedance from scalp channels was kept below 5 kΩ throughout the experiment per recommendation of the manufacturer. The EEG signal was

referenced to site FCz during recording and filtered online with a built-in 0.1 ~ 250 Hz bandpass filter. The EEG sampling (5 kHz) was synchronized with the scanner's internal clock, a step important for the proper removal of the gradient artifacts in subsequent preprocessing.

The initial EEG preprocessing was performed in BrainVision Analyzer 2.0 (Brain Products). Gradient artifact and ballistocardiogram (BCG) were corrected according to a modified version of the average artifact subtraction (AAS) method proposed in Allen et al. (1998, 2000). Specifically, the gradient artifact was corrected by first constructing an average artifact template over 41 consecutive volumes in a sliding-window fashion and then subtracting it from the raw EEG data. The BCG was removed using a similar approach in which R-waves were first detected and 21 consecutive ECG segments defined around the R-waves were averaged to produce a BCG artifact template. The resulting artifact templates were then subtracted from EEG data to correct for BCG contamination. The MR-corrected EEG data were bandpass filtered from 0.1 to 50 Hz and downsampled to 250 Hz before being exported to EEGLAB (Delorme and Makeig, 2004) for further analyses.

The continuous EEG data were epoched 500 ms before to 1500 ms after cue onset, according to two experimental conditions, i.e., attend-left and attend-right. Only trials with correct responses were included. Epochs were visually inspected for artifact contamination and trials containing excessive body motion or eye movement related artifacts were rejected. The mean trial rejection rate was 9.5%. The average number of artifact-free trials was 67 and 66 for attend left and attend right conditions, respectively, for each subject. Further EEG preprocessing using Second-Order Blind Identification

(SOBI) (Belouchrani et al., 1993) was applied to correct for any residual BCG, eye-blinking, and movement related artifacts. To sharpen spatial localization, the artifact-removed scalp voltage data was converted into reference-free current source density (CSD) data by calculating a 2-D spatial Laplacian (Mitzdorf 1985; Chen et al., 2011).

4.2.4 fMRI Acquisition and Preprocessing

MR images were acquired using a 3T Philips Achieva scanner (Philips Medical Systems) equipped with a 32-channel head coil. Functional images were collected during the experimental sessions using an echo-planar imaging (EPI) sequence with the following scanning parameters: repetition time (TR), 1.98 s; echo time (TE), 30 ms; flip angle, 80˚; field of view, 224 mm; slice number, 36; voxel size, 3.5 × 3.5 × 3.5 mm; matrix size, 64 × 64. The slices were oriented parallel to the plane connecting the anterior and posterior commissures. Image acquisition was performed during the initial 1.85 s within each EPI volume, leaving an interval of 130 ms towards the end of each TR where no image acquisition was performed. This acquisition approach enables online visual monitoring of EEG acquisition during the period not contaminated by gradient artifacts.

MRI data were processed in SPM5 (http://www.fil.ion.ucl.ac.uk/spm/). Preprocessing steps included slice timing correction, realignment, spatial co-registration, normalization, and smoothing. Slice timing correction was carried out using sinc interpolation to correct for differences in slice acquisition time within an EPI volume. The images were then spatially realigned to the first image of each session by a 6-parameter rigid body spatial transformation to account for head movement during acquisition. Each subject's images were then normalized and registered to the Montreal Neurological

Institute (MNI) space. All images were further resampled to a voxel size of 3 × 3 × 3 mm and spatially smoothed using a Gaussian kernel with 8 mm full width at half maximum (FWHM). Slow temporal drifts in baseline were removed by applying a high-pass filter with cutoff frequency set at 1/128 Hz. Global effects were accounted for by using the proportional scaling approach which divides each voxel by the spatial average of signals from all cerebral voxels (Fox et al., 2009).

4.2.5 EEG Spectral Analysis

EEG power spectral density (PSD) was calculated on CSD data from 500 ms-1000 ms after cue onset (Figure 4-2A) using the FFT-based periodogram approach. To average the power spectrum across subjects, the power spectrum from each subject was normalized by dividing the PSD by that subject's mean alpha power from the attend-left condition. Such normalization was not done when correlating alpha power with the BOLD signal. For each subject, trial-by-trial spectral power in the alpha band was calculated by integrating the unnormalized single-trial power spectrum within the range of 8 to 12 Hz in regions of interests (ROIs) over occipitoparietal sites where alpha showed the strongest attentional effects (Figure 4-2B and 4-2C; left hemisphere: O1 and P3; right hemisphere: O2 and P8). For trials rejected during preprocessing because of EEG artifacts, we used the mean alpha power calculated within the same condition as substitutes, to allow for regression with trial-by-trial BOLD activity in subsequent EEG-informed fMRI analysis (Novitskiy et al., 2011).

To measure alpha asymmetry, a single-trial alpha hemispheric lateralization index was defined as (Thut et al., 2006):

$$\mathrm{Index}(\alpha) = \frac{\alpha_{\text{Ipsilateral ROI}} - \alpha_{\text{Contralateral ROI}}}{mean(\alpha_{\text{All ROIs from every condition}})}. \quad (4\text{-}1)$$

The above lateralization index measures the percentage difference between single-trial alpha amplitudes from ROIs ipsilateral and contralateral to the attended visual field. The index is positive in general with larger values indicating stronger lateralization of alpha due to attention.

4.2.6 EEG-informed fMRI Analysis

The coupling between alpha and BOLD was examined using general linear models (GLMs). In total, seven task-related regressors were included in the GLM: Two regressors separately modeled BOLD activities related to leftward and rightward cues with correct responses, two additional regressors modeled BOLD responses to target stimuli appearing on the left and right visual fields, a fifth regressor was added to model trials with incorrect responses, and finally, trials for the “choice” condition were also modeled but not analyzed in the current study.

Coupling effects between alpha attentional modulation and BOLD was introduced into the GLM by adding parametric modulations on regressors modeling the cues. Three separate GLMs were constructed for this purpose. The first two GLMs each included a single set of parametric modulations on the cue regressors to model the coupling effects from contralateral and ipsilateral alpha, respectively. In this case, new regressors were generated in the attend left and right conditions with the height of the stick functions modeling each trial scaled by mean removed single-trial alpha power sampled from the contralateral or ipsilateral ROIs. To model the interaction between BOLD and the degree of alpha hemispheric lateralization, a single parametric modulation from the trial-

to-trial alpha lateralization index was introduced to the third GLM on regressors modeling the cues. All task-relevant regressors were convolved with a canonical hemodynamic response function (HRF) to allow for comparisons with the recorded BOLD signal. Six movement-related regressors were further incorporated into the design matrix to regress out residual signal variance from head movement.

At the individual subject level, the coupling between BOLD and alpha modulation was assessed by examining, via t-contrasts, the significance of the coefficients related to the regressors with alpha power modulations. At the group level systematic alpha-BOLD coupling was assessed via a second-level random effects analysis using a one-sample t-test. The group-level cue-evoked fMRI activations were thresholded at $p < 0.05$ corrected for multiple comparisons by controlling the false discovery rate (FDR). For alpha-BOLD coupling analysis, as it detects linear dependency between alpha and the residual fluctuation in BOLD on top of the task-evoked effects, the group-level statistical parametric maps were thresholded at $p < 0.001$, uncorrected. A cluster-level threshold of $k = 5$ voxels was further imposed. The selection of the statistical threshold for group level random effects analysis was in line with recent EEG-informed fMRI analysis (Laufs et al., 2003; Debener et al., 2005; Eichele et al., 2005; Scheeringa et al., 2011; Liu et al., 2012a).

4.3 Results

Thirteen subjects performed the task according to instructions. The mean accuracy rates, defined as the ratio between the number of correctly performed trials and the total number of trials, were 85.4% and 86.0% for attend left and attend right conditions, respectively.

4.3.1 Attentional Modulation of Alpha

For the analysis window chosen (500 – 1000 ms), posterior alpha on both hemispheres was lower than the pre-cue baseline (500 ms) (Figure 4-2B), with stronger decrease in alpha power over the scalp region contralateral to the attended hemifield (Figure 4-2A; left hemisphere: $t(12) = -2.1462$, $p < 0.05$; right hemisphere: $t(12) = -1.9145$, $p < 0.05$). Topographically, the difference in the degree of alpha suppression between two hemispheres gave rise to the hemispheric lateralization pattern seen in Figure 4-2C, in which alpha power from the attend-right condition was subtracted from the attend-left condition.

4.3.2 BOLD Activations Evoked by the Cue

The cue evoked significant BOLD activations within the dorsal attention network, including bilateral frontal eye fields (FEF), intraparietal sulci (IPS), and regions within the superior parietal lobule (SPL) (Figure 4-2D). This activation pattern, in conjunction with the post-cue lateralization of alpha, indicated that participants properly allocated their covert attention according to instructions. Other regions activated during the anticipatory period included the supplementary motor area (SMA), precuneus, and regions in the occipital lobe near area MT+ (Table 4-1).

4.3.3 BOLD-Alpha Coupling: Negative Correlations

Combining attend-left and attend-right conditions, the contralateral alpha was negatively correlated with BOLD in bilateral IPS, left middle frontal gyrus (MFG), left ventral occipital cortex (VO), and right inferior and middle temporal gyrus (IT/MTG). Relaxing the statistical threshold to $p < 0.005$, uncorrected, regions in the calcarine sulcus (CaS), bilateral VO, and bilateral crus II regions of the cerebellum further showed

negative correlation with contralateral alpha (Figure 4-3A; Table 4-2). For ipsilateral alpha fewer regions showed negative BOLD-alpha correlation (Figure 4-3B; Table 4-2). In addition, the activated voxels in the left and right IPS clusters were 42 and 4 for ipsilateral alpha, compared to 80 and 106 for contralateral alpha, suggesting that the coupling between IPS and ipsilateral alpha is weaker. It is worth noting that no coupling was observed between alpha and FEF.

4.3.4 BOLD-Alpha Coupling: Positive Correlations

For contralateral alpha, areas showing positive BOLD-alpha correlation included regions within the post-central gyrus (postCG) and anterior middle temporal gyrus (MTG), whereas for ipsilateral alpha, BOLD in medial prefrontal cortex (MPFC) and adjacent cortices in the superior frontal gyrus (SFG) showed positive correlation (Figure 4-4A, B; Table 4-2). These regions were located primarily in the sensorimotor cortices or in the default mode network.

4.3.5 Coupling between Alpha Lateralization Index and BOLD

Analysis above focuses on alpha in individual hemispheres. The degree of alpha lateralization, defined as ipsilateral alpha minus contralateral alpha, assesses the alpha difference between the two hemispheres and is an important indicator of attention control with greater alpha lateralization signifying more efficient attention control (Thut et al., 2006; Händel et al., 2011). Correlating the trial-by-trial alpha lateralization index with BOLD activity, we found positive correlation between alpha lateralization index and BOLD activity in regions within the dorsal anterior cingulate cortex (dACC) as well as adjacent areas of MPFC and superior frontal gyrus (SFG) (Figure 4-5; Table 4-2). These regions, especially dACC have been hypothesized to be part of a core or task

control network responsible for maintaining executive control over the ongoing task (Dosenbach et al., 2006). No region was found to be negatively coupled with the alpha lateralization index.

4.4 Discussion

Top-down attentional control enhances the processing of attended stimuli by biasing the sensory cortices before stimulus onset. The lateralization of alpha oscillations is a manifestation of this biasing action in both visual (Worden et al., 2000; Sauseng et al., 2005; Thut et al., 2006) and somatosensory domains (Anderson and Ding, 2011; Haegens et al., 2011). The present work examined the brain structures that contribute to the modulation of visual alpha oscillations during anticipatory attention by recording simultaneous EEG-fMRI from human subjects performing a cued spatial visual attention task. Correlating hemispheric alpha power and cross-hemisphere alpha lateralization with concurrently recorded BOLD, we showed that (1) alpha decrease was mainly associated with BOLD increases in bilateral IPS and visual areas, (2) alpha decrease was also associated with BOLD decreases in the sensorimotor cortices and the default mode network, and (3) the degree of alpha lateralization was positively coupled with BOLD in dACC.

4.4.1 Alpha and Dorsal Attention Network

During spatial visual attention, alpha is generally decreased over posterior scalp regions contralateral to the direction of attention, reflecting increased visual cortical excitability and a readiness to process sensory input (Sauseng et al., 2005; Thut et al., 2006; Grent-’t-Jong et al., 2011; Rajagovindan and Ding, 2011). One putative source of attentional modulation of alpha is the dorsal attention network, which is hypothesized to

generate and maintain a top-down expectation signal to selectively bias visual cortical activity (Corbetta and Shulman, 2002). Here, we provided further evidence showing that, along with visual cortices, increased BOLD in bilateral IPS was found to be coupled with desynchronized alpha on both ipsilateral and contralateral hemispheres during the anticipatory period. Our result, obtained nonperturbatively, is consistent with two recent studies employing rTMS showing disrupted posterior alpha desynchronization following interference of preparatory activities in FEF and IPS, core regions within the dorsal attention network (Capotosto et al., 2009, 2012).

Whether successful attention allocation is largely achieved by an enhancement of task-relevant visual cortices or a suppression of task-irrelevant areas is still debated. Evidence in terms of anticipatory alpha is mixed with some studies observing decreased alpha contralateral to the attended location (Sauseng et al., 2005; Thut et al., 2006) while others document primarily an alpha increase contralateral to the unattended location (Worden et al., 2000; Yamagishi et al., 2003; Kelly et al., 2006). In the present study, we observed alpha decreases on both hemispheres with respect to the baseline, with stronger decrease in the contralateral hemisphere. The stronger negative coupling between contralateral alpha and BOLD in IPS, compared to ipsilateral alpha, appears to suggest that top-down attentional mechanisms operated mainly by enhancing neuronal activities within task-relevant visual cortices (Corbetta and Shulman, 2002). However, unlike the paradigm used in the present study, alpha increases over areas contralateral to the unattended locations are often observed in tasks demanding active suppression of distractors at unattended locations (Yamagishi et al., 2003; Kelly et al., 2006). Therefore, a plausible explanation for the discrepancy is that the control of alpha is

mediated by the task demand and stimulus content at the to-be-ignored location with different degrees of task difficulty engaging different levels of alpha modulation on each hemisphere (Kelly et al., 2006).

4.4.2 Alpha and Task-Irrelevant Networks

Posterior alpha in the current study is found to be positively correlated with BOLD in sensorimotor cortices as well as regions within the default mode network, meaning that elevated visual cortical excitability, as indicated by decreased posterior alpha, is accompanied by decreased activities within task-irrelevant cortices in other sensory or cognitive modalities. This positive coupling suggests that attention to the visual domain disengages networks in other task-irrelevant domains to protect the ongoing visual task. Such a “push-pull” mechanism has been observed in past studies mainly in relation to sensory modalities (Klimesch, 2007; Jensen and Mazaheri, 2010). For example, visual alpha is found to be increased when attention is directed to the somatosensory (Haegens et al., 2010; Anderson and Ding, 2011) or the auditory domains (Foxe et al., 1998; Fu et al., 2001; Bollimunta et al., 2008). Higher levels of alpha activity within visual cortices were associated with enhanced performance toward auditory stimuli (Bollimunta et al., 2008). The current study extends this mechanism to include the default mode network which is known to mediate non-sensory self-referential processes (Buckner et al., 2008). Note that even in resting-state, during which external task level is kept at the minimum, a positive coupling between spontaneous visual alpha fluctuations and BOLD in the default network was reported, demonstrating an intrinsic dynamic interaction between differential cortical systems (Mayhew et al., 2013; Mo et al., 2013).

4.4.3 Differential Roles of IPS and FEF in Controlling Alpha

A somewhat surprising finding is that alpha power was not coupled with BOLD in FEF, suggesting differential roles of FEF and IPS in modulating visual alpha. This finding is consistent with a recent dynamic causal modeling study showing direct modulation of the visual cortex by IPS instead of FEF (Vossel et al., 2012). Further, rTMS on IPS, but not FEF, has been shown to induce a paradoxical increase in alpha during anticipatory attention (Capotosto et al., 2009). Taken together, the coupling between IPS and visual alpha found in our study might suggest that IPS, in contrast to FEF, engages in directly modulating visual cortical excitability. Although a host of studies have reported involvement of FEF in modulating visual cortices during attention (Ruff et al., 2006, 2008; Bressler et al., 2008; Capotosto et al., 2009), it is possible that such involvement reflects an indirect engagement of FEF in modulating visual cortices, through changes in inter-regional EEG synchrony rather than regional alpha desynchronization (Sauseng et al., 2005, 2011).

4.4.4 The Role of dACC in Anticipatory Visual Attention

When comparing two hemispheres, the degree of alpha lateralization is positively coupled with BOLD activity in dACC, and the coupling is not spatially selective, in that higher activity in dACC is associated with increased alpha lateralization regardless of the direction of attention. To date, the exact role of dACC in visual anticipatory attention is largely unknown, despite prior studies documenting its involvement in tasks requiring voluntary attentional orienting (Shulman et al., 2003; Fan et al., 2007; Aarts et al., 2008; Corbetta et al., 2008). Studies examining dACC's function across multiple task domains suggest that dACC is part of a "core system" or "task control network" engaging in

maintaining a global task-set to mediate goal-directed behavior (Dosenbach et al., 2006, 2007, 2008; Corbetta et al., 2008; Sakai, 2008). This network, containing dACC and bilateral anterior insula (aI), is hypothesized to independently send out top-down signals to other domain-specific executive areas to ensure the proper allocation of resources to support various task-specific behaviors (Shulman et al., 2003; Crottaz-Herbette and Menon, 2006; Dosenbach et al., 2006; Walsh et al., 2010; Wen et al., 2012). Within the domain of attentional control, although alpha on each individual hemisphere might show divergent patterns of synchronization and desynchronization, studies have proposed that the global allocation of attentional resources is reflected in the lateralization of alpha over two hemispheres (Thut et al., 2006; Händel et al., 2011). Hence, the positive correlation between BOLD in dACC and alpha lateralization found in the current study is key evidence indicating that dACC maintains the "attentional-set" during target anticipation and mediates attentional deployment to facilitate overall task performance.

4.4.5 Summary

The current study contributes to our understanding of the top-down mechanisms of attention by providing nonperturbative evidence demonstrating the involvement of frontoparietal attention and executive regions in modulating posterior alpha oscillations during anticipatory attention. It also distinguishes the differential roles of parietal and frontal regions in modulating posterior alpha and the topological organization of the top-down mechanisms. By identifying regions positively coupled with posterior alpha, this study further provides evidence suggesting a mechanism of active inhibition over task-irrelevant sensory and cognitive modalities (Klimesch et al., 2007). Finally, by combining imaging modalities, a role of dorsal ACC in anticipatory attentional control is suggested.

Table 4-1. Event-related activations following cue onset

Anatomical Regions	Hemisphere	MNI Coordinates (x,y,z)	Z-score
Frontal Eye Field	Left	-24, -3, 57	3.56
	Right	39, 0, 57	4.15
Intraparietal Sulcus	Left	-33, -48, 42	4.10
	Right	27, -57, 51	5.13
MT+	Left	-48, -69, -15	5.25
	Right	51, -72, -12	5.24
Precuneus	Left	-6, -57, 57	3.78
	Right	6, -54, 54	3.98
Supplementary Motor Area	Left	-9, 12, 51	3.16

Table 4-2. Coupling between alpha and BOLD with attend left and right combined

Anatomical Regions	Hemisphere	MNI Coordinates (x,y,z)	Z-score
Negative coupling between BOLD and contralateral alpha			
Intraparietal Sulcus	Left	-33, -69, 57	4.81
	Right	39, -51, 54	4.33
Inferior and Middle Temporal Gyrus	Right	60, -33, -15	4.21
Middle Frontal Gyrus	Left	-39, 42, 33	3.71
Ventral Occipital Cortex	Left	-35, -81, -17	4.17
	Right	42, -84, -15	3.25*
Calcarine Sulcus		9, -87, 0	3.65*
Crus II of Cerebellum	Left	-12, -81, -39	4.35
	Right	3, -81, -33	2.88*
Negative coupling between BOLD and ipsilateral alpha			
Intraparietal Sulcus	Left	-30, -63, 39	4.01
	Right	36, -63, 51	3.42
Crus II of Cerebellum	Left	-21, -75, -42	3.41
Positive coupling between BOLD and contralateral alpha			
Post-central Gyrus	Left	-48, -12, 24	4.59
	Right	60, -12, 39	4.48
Middle Temporal Gyrus	Left	-57, -9, -18	3.67
Positive coupling between BOLD and ipsilateral alpha			
Medial Prefrontal Cortex	Right	15, 48, 33	4.47
Positive coupling between BOLD and alpha lateralization index			
Dorsal Anterior Cingulate Cortex	Right	6, 24, 39	3.45
Medial Prefrontal Cortex	Right	15, 51, 27	3.92
Superior Frontal Gyrus	Left	-21, 36, 39	3.69

*: $p < 0.005$.

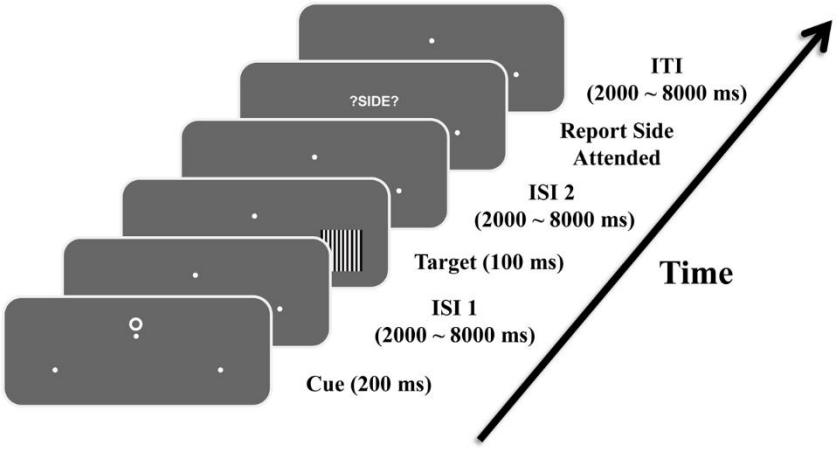

Figure 4-1. An illustration of the sequence of events within a trial. Following cue onset, participants covertly directed their attention toward either left of right hemifield while maintaining eye fixation on the central point. Targets were flashed briefly at one of the marked locations after a variable inter-stimulus interval. Participants were required to discriminate the thickness of the stripes and make a forced 2-button choice only when targets appeared on the attended location. At the end of each trial, participants were also prompted to report the hemifield they attended to.

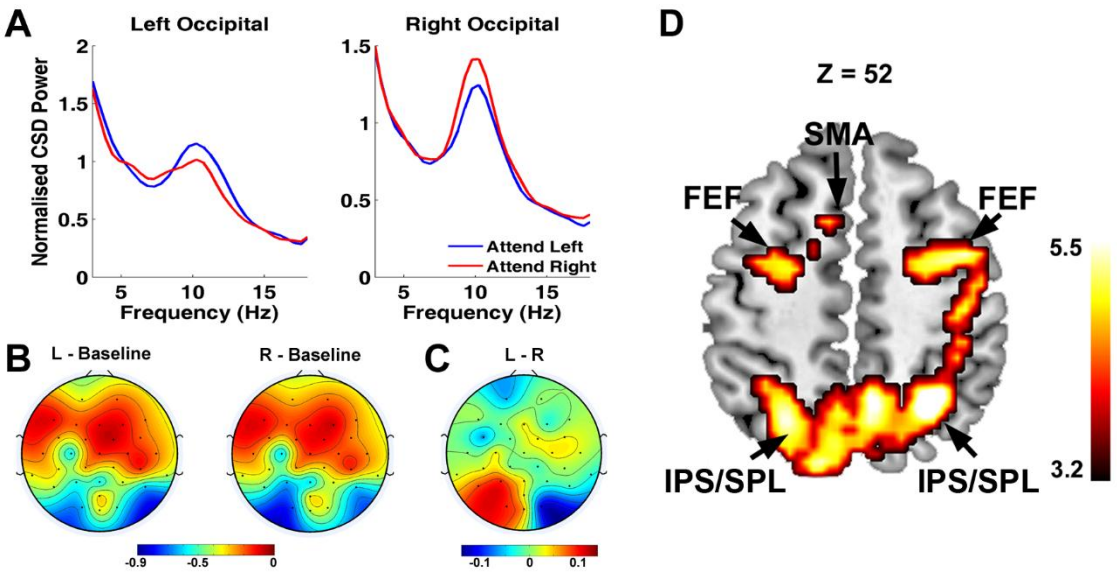

Figure 4-2. Attentional modulation of alpha power and BOLD. A) Grand average power spectral density from occipital channels (O1 and O2) showing modulation in the alpha frequency band (8 – 12 Hz) during 500 – 1000 ms after cue onset. B) Scalp topography showing alpha desynchronization during Attend Left and Attend Right, respectively. C) Difference topography between Attend Left and Attend Right showing alpha asymmetry during covert shifting of attention. D) BOLD activation showing the engagement of dorsal attention network during the post-cue anticipatory period. Activation map is plotted according to the neurological convention with left shown on the left side. FEF: frontal eye field; IPS: intraparietal sulcus; SPL: superior parietal lobule; SMA: supplementary motor area.

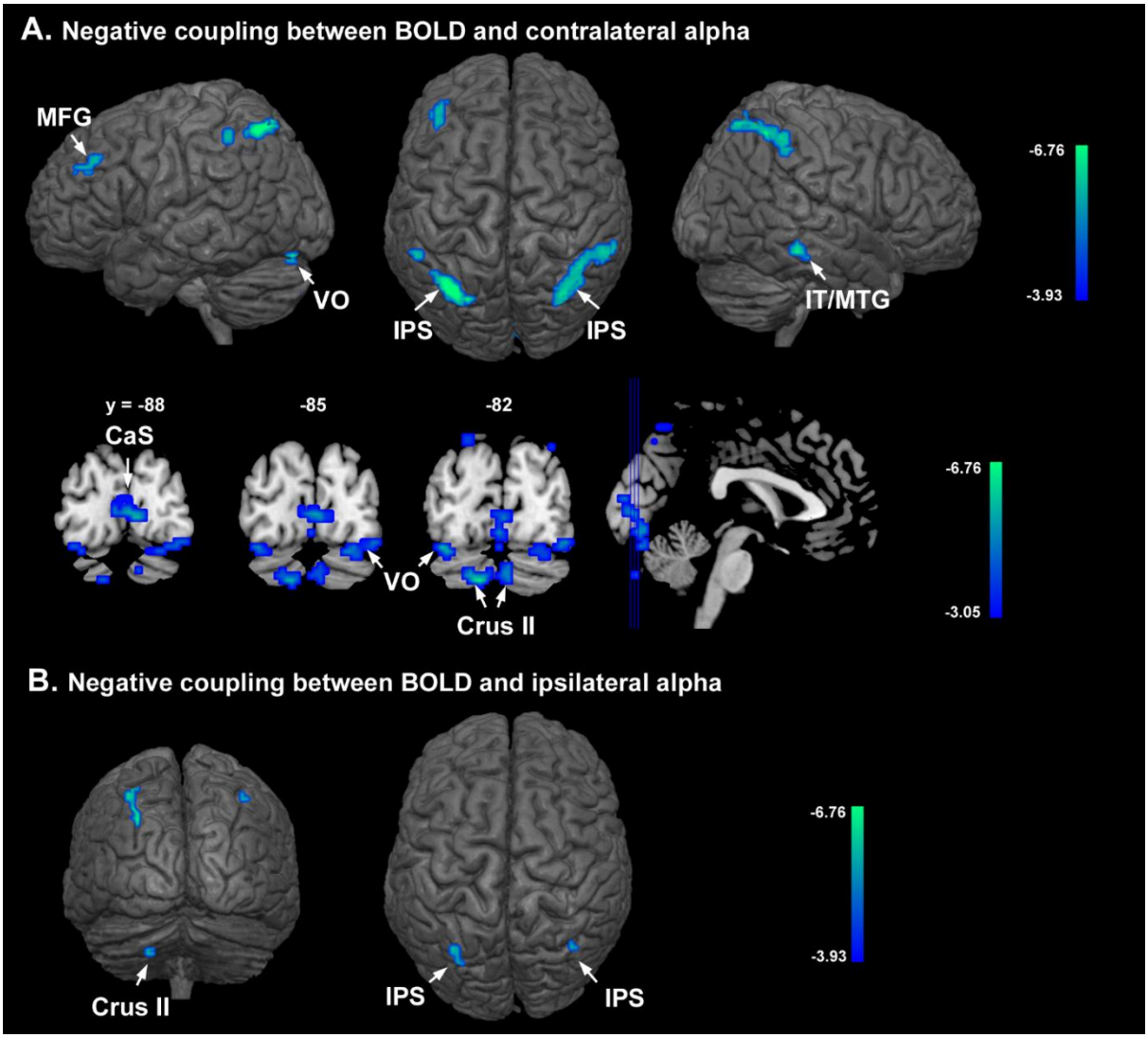

Figure 4-3. Negative coupling between BOLD and alpha with Attend Left and Right combined. A) Regions exhibiting negative coupling with contralateral alpha during voluntary attention (top-row and middle tow correspond to $p < 0.001$ and $p<0.005$, uncorrected, respectively). B) Regions showing negative coupling between BOLD and ipsilateral alpha ($p < 0.001$, uncorrected). IPS: intraparietal sulcus; MFG: middle frontal gyrus; IT: inferotemporal gyrus; MTG: middle temporal gyrus; VO: ventral occipital cortex; CaS: calcarine sulcus; Crus II: crus II of cerebellum.

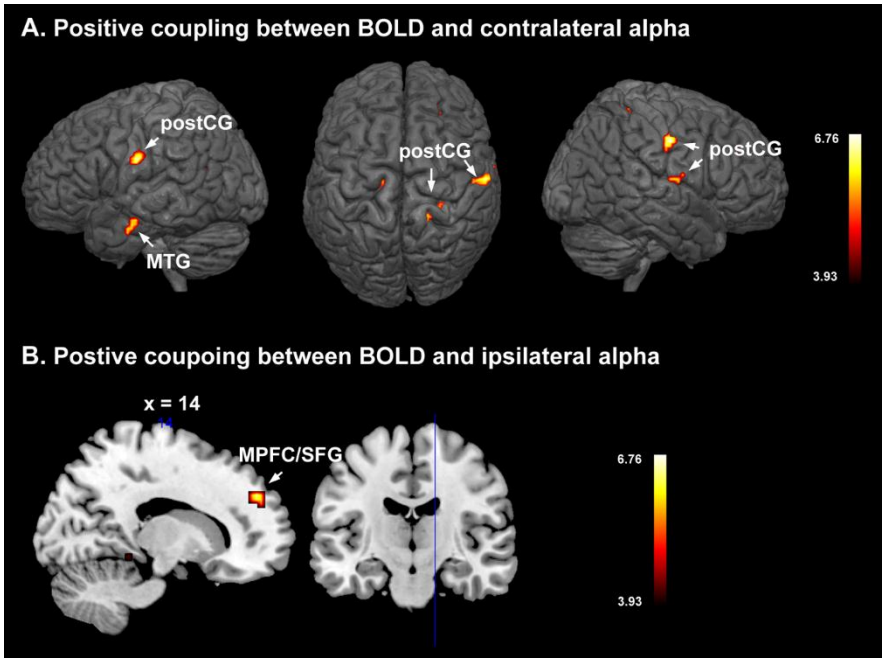

Figure 4-4. Positive coupling between BOLD and A) contralateral alpha and B) ipsilateral alpha with Attend Left and Right combined. The statistical parametric maps are thresholded at $p < 0.001$, uncorrected. MPFC: medial prefrontal cortex; MTG: middle temporal gyrus; postCG: post-central gyrus; SFG: superior frontal gyrus.

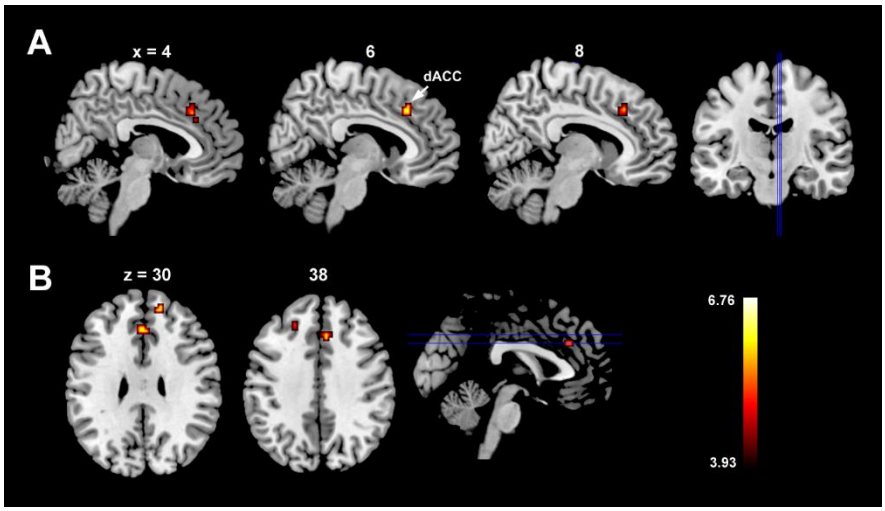

Figure 4-5. Coupling between BOLD and alpha lateralization index. A) Sagittal slices showing a region in dorsal anterior cingulate cortex (dACC) which is positively correlated with alpha lateralization. B) Coronal slices showing the same region in dACC along with adjacent regions in superior frontal sulcus (SFS) and medial prefrontal cortex (MPFC).

CHAPTER 5
CONCLUSIONS

Neurophysiological signals contain a substantial amount of variability across multiple repeated experimental trials. Traditionally, researchers treat such trial-to-trial variability as task-irrelevant noises and the corresponding ensemble averaging procedure tends to average out such variability. However, recent studies have shown that the trial-to-trial variability bears important information about the dynamics of the underlying cognitive processes (Chen et al., 2006). The simple ensemble averaging procedure cannot resolve such detailed information. Therefore, single-trial estimation techniques provide a promising tool to analyzing the trial-to-trial variability inherent in neurophysiological signals. This dissertation employed a recently developed single-trial analysis algorithm, ASEO (Xu et al., 2009), to study the functional implications associated with the trial-to-trial variability in both the EEG and BOLD domain along three studies.

In the first study, we sought to study the trial-by-trial dynamics of the sensory facilitation process during classical aversive conditioning. We for the first time characterized the detailed temporal dynamics of the learning process within a conditioning block by estimating and comparing the trial-by-trial evolving patterns of single-trial P1 amplitudes between CS+ and CS–. Specifically, three distinct phases of P1 modulation as a function of experimental trials were identified as conditioning progresses, with P1 amplitude showing differential modulating patterns between CS+ and CS– within each phase. In contrast to a prior study employing traditional ERP measures that reported no conditioning-related modulation of P1 (Stolarova et al., 2006), the difference in temporal dynamics of P1 amplitudes found in this study between the

CSs was a strong indication that conditioning modulates neuronal activities in the extrastriate cortex, albeit in a complex way. Moreover, the fact that P1 amplitudes showed a complex trial-to-trial temporal dynamics in the conditioning block suggests that prior emotional experience acts to increase both the reactivity and efficiency of sensory cortices, possibly in a sequential way with the increase phase reflecting increased reactivity and the final habituating phase reflecting enhanced network efficiency. Such temporal dynamics of sensory modulation is further in line with the prediction error theory of attention during conditioning (Pearce and Hall, 1980), which predicts that subjects' level of attention tends to decrease if the level of uncertainty decreases, leading to facilitation of increasingly early stages of visual processing as learning progresses (Keil, 2004). Given that the extrastriate cortex receives re-entrant projections from the amygdala (Amaral and Price, 1984), it is likely that the preferential sensory sensitization toward CS+ originated from such re-entrant modulations from the amygdala, which has also been found to exhibit habituation after repeated CS-presentations (Büchel and Dolan, 2000).

In the second study, we incorporated ASEO single-trial ERP estimation with EEG-informed fMRI analysis to investigate brain structures contributing to the scalp-recorded LPP. Areas contributing to either the generation or modulation of LPP were identified by testing for significant correlations between single-trial LPP amplitudes with concurrently measured single-trial BOLD activities throughout the entire brain. We found that areas positively correlated with LPP amplitude consisted of both the visual cortex and other areas known to be involved in emotional processing, such as the orbitofrontal cortex, insula, and amygdala. This suggests that emotional processing naturally attracts

processing resources and activates an extensive network reflecting the engagement of the fundamental motivation system. Restricting our analyses into positive and negative categories of emotions, we found categorical-specific differences in regions showing LPP and BOLD coupling, which indicates that the underlying structures giving rise to the LPP differ across emotion categories despite they all elicit the LPP with similar temporal dynamics and scalp topography.

It is worth noting that prior studies have attempted to locate the potential generators of the LPP using EEG source localizing techniques (Keil et al., 2002; Sabatinelli et al., 2007b). Yet these studies were only partly successful because EEG source localizing techniques in general have relatively low spatial resolution and more importantly, it could not resolve information coming from distant subcortical structures which are usually critical in emotional processing. Recent studies have also examined this problem by correlating LPP with fMRI acquired from a separate experimental session in a cross-subjects fashion (Sabatinelli et al., 2007b, 2013). One potential drawback of such an approach is that it is difficult to control the psychological and biological conditions to be exactly the same in different recording session. In addition, the correlation between the average LPP across subjects and BOLD does not reflect their trial-by-trial co-variations in a within-subjects fashion. Given the above, the single-trial estimation combined with simultaneous EEG-fMRI employed in this study was capable of overcoming these limitations and was proven useful in revealing brain areas contributing to scalp-recorded EEG features.

Finally in the third study, we identified cortical areas contributing to two aspects of the trial-to-trial attentional modulation of posterior alpha, desynchronization and

hemispheric lateralization, via the EEG-informed fMRI analysis similar to that employed in the second study. Main regions modulating posterior alpha desynchronization during attention was found to include bilateral intraparietal sulci (IPS) and the left middle frontal gyrus (MFG), core regions within the attention system. Yet interestingly, the frontal eye field, also being part of the dorsal attention network, was not found to contribute to alpha desynchronization, suggesting differential roles of frontal and parietal regions in modulating posterior alpha. The fact that a stronger negative coupling was found between BOLD and contralateral alpha, compared to ipsilateral alpha, suggests that top-down attentional mechanisms operated mainly by enhancing neuronal activities within task-relevant visual cortices. On the other hand, regions within the sensorimotor cortices and the default mode network showed positive coupling with alpha, suggesting a mechanism of active inhibition over task-irrelevant networks. Last but not least, the alpha hemispheric lateralization was correlated with BOLD activity in the dorsal anterior cingulate cortex (dACC) for both attend left and right conditions, providing key evidence indicating the dACC's role in maintaining a global attentional-set to facilitate overall deployment of attentional resources among task- relevant and irrelevant cortices.

LIST OF REFERENCES

Aarts E, Roelofs A, van Turennout M (2008) Anticipatory activity in anterior cingulate cortex can be independent of conflict and error likelihood. J Neurosci, 28:4671-4678.

Adolphs R (2002) Neural systems for recognizing emotion. Curr Opin Neurobiol 12:169–177.

Aharon I, Etcoff N, Ariely D, Chabris CF, O'Connor E, Breiter HC (2001) Beautiful faces have variable reward value: fMRI and behavioral evidence. Neuron 32:537–551.

Allen PJ, Josephs O, Turner R (2000) A method for removing imaging artifact from continuous EEG recorded during functional MRI. Neuroimage 12:230–239.

Allen PJ, Polizzi G, Krakow K, Fish DR, Lemieux L (1998) Identification of EEG events in the MR scanner: the problem of pulse artifact and a method for its subtraction. Neuroimage 8:229–239.

Alves NT, Fukusima SS, Aznar-Casanova A (2008) Models of brain asymmetry in emotional processing. Psychol Neurosci 1:63–66.

Amaral DG, Price JL (1984) Amygdalo-cortical projections in the monkey (macaca fascicularis). J Comp Neurol 230:465–496.

Amir N, Beard C, Cobb M, Bomyea J (2009) Attention modification program in individuals with generalized anxiety disorder. J Abnorm Psychol 118:28–33.

Anderson KL, Ding M (2011) Attentional modulation of the somatosensory mu rhythm. Neuroscience 180:165–180.

Anderson KL, Rajagovindan R, Ghacibeh GA, Meador KJ, Ding M (2010) Theta oscillations mediate interaction between prefrontal cortex and medial temporal lobe in human memory. Cereb Cortex 20:1604–1612.

Astafiev SV, Shulman GL, Stanley CM, Snyder AZ, Essen DCV, Corbetta M (2003) Functional organization of human intraparietal and frontal cortex for attending, looking, and pointing. J Neurosci 23:4689–4699.

Bartnik EA, Blinowska KJ, Durka PJ (1992) Single evoked potential reconstruction by means of wavelet transform. Biol Cybern 67:175–181.

Belouchrani A, Abed-Meraim K, Cardoso JF, Moulines E (1993) Second order blind separation of temporally correlated sources. Proc Int Conf on Digital Sig Proc, pp. 346–351, Cyprus.

Bénar C, Schön D, Grimault S, Nazarian B, Burle B, Roth M, Badier J, Marquis P, Liegeois-Chauvel C, Anton J (2007) Single-trial analysis of oddball event-related potentials in simultaneous EEG-fMRI. Hum Brain Mapp 28:602–613.

Bollimunta A, Chen Y, Schroeder CE, Ding M (2008) Neuronal mechanisms of cortical alpha oscillations in awake-behaving macaques. J Neurosci 28:9976–9988.

Bradley MM (2009) Natural selective attention: orienting and emotion. Psychophysiology 46:1–11.

Bradley MM, Lang PJ (1994) Measuring emotion: the self-assessment manikin and the semantic differential. J Behav Ther Exp Psychiatry 25:49–59.

Bradley MM, Sabatinelli D, Lang PJ, Fitzsimmons JR, King W, Desai P (2003) Activation of the visual cortex in motivated attention. Behav Neurosci 117:369–380.

Breiter H, Etcoff N, Whalen P, Kennedy W, Rauch S, Buckner R, Strauss M, Hyman S, Rosen B (1996) Response and habituation of the human amygdala during visual processing of facial expression. Neuron 17:875–887.

Bressler SL, Tang W, Sylvester CM, Shulman GL, Corbetta M (2008) Top-down control of human visual cortex by frontal and parietal cortex in anticipatory visual spatial attention. J Neurosci 28:10056 –10061.

Buckner RL, Andrews-Hanna JR, Schacter DL (2008) The brain's default network. Annals of the New York Academy of Science, 1124:1-38.

Büchel C, Coull JT, Friston KJ (1999a) The predictive value of changes in effective connectivity for human learning. Science 283:1538–1541.

Büchel C, Dolan RJ, Armony JL, Friston KJ (1999b) Amygdala-hippocampal involvement in human aversive trace conditioning revealed through event-related functional magnetic resonance imaging. J Neurosci 19:10869–10876.

Büchel C, Dolan RJ (2000) Classical fear conditioning in functional neuroimaging. Curr Opin Neurobiol 10:219–223.

Büchel C, Morris J, Dolan RJ, Friston KJ (1998) Brain systems mediating aversive conditioning: an event-related fMRI study. Neuron 20:947–957.

Cacioppo JT, Crites SL Jr, Berntson GG, Coles MGH (1993) If attitudes affect how stimuli are processed, should they not affect the event-related brain potential? Psychol Sci 4:108–112.

Cacioppo JT, Crites SL Jr, Gardner WL, Bernston GG (1994) Bioelectrical echoes from evaluative categorizations: I. A late positive brain potential that varies as a function of trait negativity and extremity. J Pers Soc Psychol 67:115–125.

Capotosto P, Babiloni C, Romani GL, Corbetta M (2009) Frontoparietal cortex controls spatial attention through modulation of anticipatory alpha rhythms. J Neurosci 29:5863–5872.

Capotosto P, Babiloni C, Romani GL, Corbetta M (2012) Differential contribution of right and left parietal cortex to the control of spatial attention: a simultaneous EEG–rTMS study. Cereb Cortex 22:446–454.

Chen Y, Bressler SL, Knuth KH, Truccolo WA, Ding M (2006) Stochastic modeling of neurobiological time series: power, coherence, Granger causality, and separation of evoked responses from ongoing activity. Chaos 16, 026113.

Chen Y, Dhamala M, Bollimunta A, Schroeder CE, Ding M (2011) Current source density analysis of ongoing neural activity: theory and application. In: Electrophysiological recording techniques, neuromethods (Vertes RP and Stackman RW, eds), pp 27–40, Totowa, NJ: Humana.

Coppola R, Tabor R, Buchsbaum MS (1978) Signal to noise ratio and response variability measurements in single trial evoked potentials. Electroencephalogr Clin Neurophysiol 44:214–222.

Corbetta M, Kincade JM, Ollinger JM, McAvoy MP, Shulman GL (2000) Voluntary orienting is dissociated from target detection in human posterior parietal cortex. Nat Neurosci 3:292–297.

Corbetta M, Shulman GL (2002) Control of goal-directed and stimulus-driven attention in the brain. Nat Rev Neurosci 3:201–215.

Corbetta M, Patel G, Shulman GL (2008) The reorienting system of the human brain: from environment to theory of mind. Neuron 58:306–324.

Costa VD, Lang PJ, Sabatinelli D, Versace F, Bradley MM (2010) Emotional imagery: Assessing pleasure and arousal in the brain's reward circuitry. Hum Brain Mapp 31, 1446–1457.

Craig AD (2009) How do you feel-now? The anterior insula and human awareness. Nat Rev Neurosci 10:59–70.

Crottaz-Herbette S, Menon V (2006) Where and when the anterior cingulate cortex modulates attentional response: combined fMRI and ERP evidence. J Cogn Neurosci 18:766-780.

Cuthbert BN, Schupp HT, Bradley MM, Birbaumer N, Lang PJ (2000) Brain potentials in affective picture processing: covariation with autonomic arousal and affective report. Biol Psychol 52:95–111.

David SP, Munafò MR, Johansen-Berg H, Smith SM, Rogers RD, Matthews PM, Walton RT (2005) Ventral striatum/nucleus accumbens activation to smoking-related pictorial cues in smokers and nonsmokers: a functional magnetic resonance imaging study. Biol Psychiatry 58: 488–494.

Debener S, Ullsperger M, Siegel M, Engel AK (2007) Towards single-trial analysis in cognitive brain research. Trends Cogn Sci 11:502–503.

Debener S, Ullsperger M, Siegel M, Fiehler K, von Cramon DY, Engel AK (2005) Trial-by-trial coupling of concurrent electroencephalogram and functional magnetic resonance imaging identifies the dynamics of performance monitoring. J Neurosci 25:11730 –11737.

Delorme A, Makeig S (2004) EEGLAB: an open source toolbox for analysis of single-trial EEG dynamics including independent component analysis. J Neurosci Methods 134:9–21.

Diamond DM, Weinberger NM (1984): Physiological plasticity of single neurons in auditory cortex of the cat during acquisition of the pupillary conditioned response: II. Secondary field (AII). Behav Neurosci 98:189–210.

DiRusso F, Martínez A, Sereno MI, Pitzalis S, Hillyard SA (2001) Cortical sources of the early components of the visual evoked potential. Hum Brain Mapp 15:95–111.

Dosenbach NUF, Fair DA, Cohen AL, Schlaggar BL, Petersen SE (2008) A dual-networks architecture of top-down control. Trends Cogn Sci 12:99–105.

Dosenbach NUF, Fair DA, Miezin FM, Cohen AL, Wenger KK, Dosenbach RAT, Fox MD, Snyder AZ, Vincent JL, Raichle ME, Schlaggar BL, Petersen SE (2007) Distinct brain networks for adaptive and stable task control in humans. Proc Natl Acad Sci 104:11073–11078.

Dosenbach NUF, Visscher KM, Palmer ED, Miezin FM, Wenger KK, Kang HC, Burgund ED, Grimes AL, Schlaggar BL, Petersen SE (2006) A core system for the implementation of task sets. Neuron 50:799–812.

Eichele T, Specht K, Moosmann M, Jongsma MLA, Quiroga RQ, Nordby H, Hugdahl K (2005) Assessing the spatiotemporal evolution of neuronal activation with single-trial event-related potentials and functional MRI. Proc Natl Acad Sci USA 102:17798 –17803.

Elbert T, Heim S (2001) A light and a dark side. Nature 411:139.

Fan J, Gu X, Liu X, Guise KG, Park Y, Martin L, de Marchena A, Tang CY, Minzenberg MJ, Hof PR (2011) Involvement of the anterior cingulate and frontoinsular cortices in rapid processing of salient facial emotional information. Neuroimage 54:2539 –2546.

Fan J, Kolster R, Ghajar J, Suh M, Knight RT, Sarkar R, McCandliss, BD (2007) Response anticipation and response conflict: an event-related potential and functional magnetic resonance imaging study. J Neurosci 27:2272-2282.

Ferretti A, Caulo M, Del Gratta C, Di Matteo R, Merla A, Montorsi F, Pizzella V, Pompa P, Rigatti P, Rossini PM, Salonia A, Tartaro A, Romani GL (2005) Dynamics of male sexual arousal: distinct components of brain activation revealed by fMRI. NeuroImage 26:1086–1096.

Ferry AT, Öngür D, An X, Price JL (2000) Prefrontal cortical projections to the striatum in macaque monkeys: Evidence for an organization related to prefrontal networks. J Comp Neurol 425:447–470.

Fogelson N, Wang X, Lewis JB, Kishiyama MM, Ding M, Knight RT (2009) Multimodal effects of local context on target detection: evidence from P3b. J Cogn Neurosci 21:1680–1692.

Foti D, Olvet DM, Klein DN, Hajcak G (2010) Reduced electrocortical response to threatening faces in major depressive disorder. Depress Anxiety 27:813–820.

Fox K, Wong RO (2005): A comparison of experience-dependent plasticity in the visual and somatosensory systems. Neuron 48:465–477.

Fox MD, Zhang D, Snyder AZ, Raichle ME (2009) The global signal and observed anticorrelated resting state brain networks. J Neurophysiol 101:3270 – 3283.

Foxe JJ, Simpson GV, Ahlfors SP (1998) Parieto-occipital approximately 10 Hz activity reflects anticipatory state of visual attention mechanisms. Neuroreport 9:3929–3933.

Friedman JH (1991) Multivariate adaptive regression splines. Ann Stat 19:1–141.

Fu, KM, Foxe JJ, Murray MM, Higgins BA, Javitt DC, Schroeder CE (2001) Attention-dependent suppression of distracter visual input can be cross-modally cued as indexed by anticipatory parieto-occipital alpha-band oscillations. Cogn Brain Res 12:145–152.

Giesbrecht B, Woldorff MG, Song AW, Mangun GR (2003) Neural mechanisms of top-down control during spatial and feature attention. NeuroImage 19:496–512.

Grent-’t-Jong T, Boehler CN, Kenemans JL, Woldorff MG (2011) Differential Functional Roles of Slow-Wave and Oscillatory-Alpha Activity in Visual Sensory Cortex during Anticipatory Visual-Spatial Attention. Cereb Cortex 21:2204-2216.

Grill-Spector K, Henson R, Martin A (2006) Repetition and the brain: neural models of stimulus-specific effects. Trends Cogn Sci 10:14–23.

Gruber T, Keil A, Müller MM (2001) Modulation of induced gamma band responses and phase synchrony in a paired associate learning task in the human EEG. Neurosci Lett 316:29–32.

Gu X, Liu X, Guise KG, Naidich TP, Hof PR, Fan J (2010) Functional dissociation of the frontoinsular and anterior cingulate cortices in empathy for pain. J Neurosci 30:3739 –3744.

Guo C, Lawson AL, Jiang Y (2007) Distinct neural mechanisms for repetition effects of visual objects. Neuroscience 149:747–759.

Guo C, Lawson AL, Zhang Q, Jiang Y (2008) Brain potentials distinguish new and studied objects during working memory. Hum Brain Mapp 29:441–452.

Haegens S, Händel BF, Jensen O (2011) Top-down controlled alpha band activity in somatosensory areas determines behavioral performance in a discrimination task. J Neurosci 31: 5197-5204.

Haegens S, Osipova D, Oostenveld R, Jensen O (2010) Somatosensory working memory performance in humans depends on both engagement and disengagement of regions in a distributed network. Hum Brain Mapp 31:26–35.

Hamann SB, Ely TD, Hoffman JM, Kilts CD (2002) Ecstasy and Agony: activation of the human amygdala in positive and negative emotion. Psychol Sci 13:135–141.

Händel BE, Haarmeier T, Jensen O (2011) Alpha oscillations correlate with the successful inhibition of unattended stimuli. J Cogn Neurosci 23:2494-2502.

Hendler T, Rotshtein P, Yeshurun Y, Weizmann T, Kahn I, Ben- Bashat D, Malach R, Bleich A (2003) Sensing the invisible: differential sensitivity of visual cortex and amygdala to traumatic context. Neuroimage 19:587–600.

Hopfinger JB, Buonocore MH, Mangun GR (2000) The neural mechanisms of top-down attentional control. Nat Neurosci 3:284–291.

Ishai A, Pessoa L, Bikle PC, Ungerleider LG (2004) Repetition suppression of faces is modulated by emotion. Proc Natl Acad Sci USA 101:9827–9832.

Jaskowski P, Verleger R (1999) Amplitudes and latencies of single-trial ERP's estimated by a maximum-likelihood method. IEEE Trans Biomed Eng 46:987–993.

Jaworska N, Thompson A, Shah D, Fisher D, Ilivitsky V, Knott V (2012) Acute tryptophan depletion effects on the vertex and late positive potentials to emotional faces in individuals with a family history of depression. Neuropsychobiology 65:28–40.

Jensen O, Mazaheri A (2010) Shaping functional architecture by oscillatory alpha activity: gating by inhibition. Front Hum Neurosci 4:186.

Jiang Y, Haxby JV, Martin A, Ungerleider LG, Parasuraman R (2000) Complementary neural mechanisms for tracking items in human working memory. Science 287:643–646.

Jiang Y, Lianekhammy J, Lawson A, Guo C, Lynam D, Joseph JE, Gold BT, Kelly TH (2009) Brain responses to repeated visual experience among low and high sensation seekers: role of boredom susceptibility. Psychiatry Res 173:100–106.

Junghöfer M, Elber T, Tucker DM, Rockstroh B (2000) Statistical control of artifacts in dense array EEG/MEG studies. Psychophysiology 37:523–532.

Karama S, Lecours AR, Leroux J, Bourgouin P, Beaudoin G, Joubert S, Beauregard M (2002) Areas of brain activation in males and females during viewing of erotic film excerpts. Hum Brain Mapp 16:1–13.

Kastner S, Pinsk MA, Weerd PD, Desimone R, Ungerleider LG (1999) Increased Activity in Human visual cortex during directed attention in the absence of visual stimulation. Neuron 22:751–761.

Keil A (2004) The role of human prefrontal cortex in motivated perception and behavior: Evidence from macroscopic electrocortical signals. In: Otani S, editor. Prefrontal Cortex: From Synaptic Plasticity to Cognition. New York: Kluwer. pp 245–267.

Keil A, Bradley MM, Hauk O, Rockstroh B, Elbert T, Lang PJ (2002) Large‐scale neural correlates of affective picture processing. Psychophysiology 39, 641–649.

Keil A, Costa V, Smith JC, Sabatinelli D, McGinnis EM, Bradley MM, Lang PJ (2012) Tagging cortical networks in emotion: a topographical analysis. Hum Brain Mapp 33:2920-2931.

Keil A, Gruber T, Müller MM, Moratti S, Stolarova M, Bradley MM, Lang PJ (2003) Early modulation of visual perception by emotional arousal: evidence from steady-state visual evoked brain potentials. Cogn Affect Behav Neurosci 3:195–206.

Keil A, Sabatinelli D, Ding M, Lang PJ, Ihssen N, Heim S (2009) Re-entrant projections modulate visual cortex in affective perception: directional evidence from Granger causality analysis. Hum Brain Mapp 30:532–540.

Keil A, Stolarova M, Moratti S, Ray WJ (2007) Adaptation in human visual cortex as a mechanism for rapid discrimination of aversive stimuli. NeuroImage 36:472–479.

Kelly SP, Lalor EC, Reilly RB, Foxe JJ (2006) Increases in alpha oscillatory power reflect an active retinotopic mechanism for distracter suppression during sustained visuo-spatial attention. J Neurophysiol 95:3844 –3851.

Kleinbaum DG, Kupper LL, Muller KE (1988) Applied Regression Analysis and Other Multivariable Methods, 2nd ed. Boston: PWS-KENT Publishing Company.

Klemm M, Haueisen J, Ivanova G (2009) Independent component analysis: comparison of algorithms for the investigation of surface electrical brain activity. Med Biol Eng Comput 47:413–423.

Klimesch W, Sauseng P, Hanslmayr S (2007) EEG alpha oscillations: the inhibition-timing hypothesis. Brain Res Rev 53:63–88.

Knuth KH, Shah AS, Truccolo WA, Ding M, Bressler SL, Schroeder CE (2006) Differentially variable component analysis: identifying multiple evoked components using trial-to-trial variability. J Neurophysiol 95:3257–3276.

Knutson B, Fong GW, Bennett SM, Adams CM, Hommer D (2003) A region of mesial prefrontal cortex tracks monetarily rewarding outcomes: characterization with rapid event-related fMRI. Neuroimage 18:263–272.

Krolak-Salmon P, Hénaff MA, Vighetto A, Bertrand O, Mauguière F (2004) Early amygdala reaction to fear spreading in occipital, temporal, and frontal cortex: a depth electrode ERP study in human. Neuron 42:665–676.

LaBar KS, Gatenby C, Gore JC, LeDoux JE (1998) Human amygdala activation during conditioned fear acquisition and extinction: a mixed-trial fMRI study. Neuron 20:937–945.

Lane RD, Reiman EM, Bradley MM, Lang PJ, Ahern GL, Davidson RJ, Schwartz GE (1997) Neuroanatomical correlates of pleasant and unpleasant emotion. Neuropsychologia 35:1437–1444.

Lang PJ, Bradley, MM (2010) Emotion and the motivational brain. Biol Psychol 84:437–450.

Lang PJ, Bradley MM, Cuthbert BN (1997a) International affective picture system (IAPS): Technical manual and affective ratings. NIMH Center for the Study of Emotion and Attention, University of Florida.

Lang PJ, Bradley MM, Cuthbert BN (1998a) Emotion, motivation, and anxiety: brain mechanisms and psychophysiology. Biol Psychiatry 44:1248–1263.

Lang PJ, Bradley MM, Cuthbert BN (2008) International affective picture system (IAPS): affective ratings of pictures and instruction manual. University of Florida, Gainesville, FL: Technical Report A-8.

Lang PJ, Bradley MM, Fitzsimmons JR, Cuthbert BN, Scott JD, Moulder B, Nangia V (1998b) Emotional arousal and activation of the visual cortex: an fMRI analysis. Psychophysiology 35:199–210.

Lang PJ, Simons RF, Balaban MT (1997b) Attention and orienting: sensory and motivational processes. Hillsdale, NJ: Erlbaum.

Lange DH, Pratt H, Inbar GF (1997) Modeling and estimation of single evoked brain potential components. IEEE Trans Biomed Eng 44:791–799.

Laufs H, Holt JL, Elfont R, Krams M, Paul JS, Krakow K, Kleinschmidt A (2006) Where the BOLD signal goes when alpha EEG leaves. Neuroimage 31:1408–1418.

Laufs H, Kleinschmidt A, Beyerle A, Eger E, Salek-Haddadi A, Preibisch C, Krakow K (2003a) EEG-correlated fMRI of human alpha activity. Neuroimage 19:1463–1476.

Laufs H, Krakow K, Sterzer P, Eger E, Beyerle A, Salek-Haddadi A, Kleinschmidt A (2003b) Electroencephalographic signatures of attentional and cognitive default modes in spontaneous brain activity fluctuations at rest. Proc Natl Acad Sci 100:11053–11058.

LeDoux J (2003) The emotional brain, fear, and the amygdala. Cell Mol Neurobiol 23:727–738.

Leutgeb V, Schäfer A, Schienle A (2011) Late cortical positivity and cardiac responsitivity in female dental phobics when exposed to phobia-relevant pictures. Int J Psychophysiol 79:410–416.

Lissek S, Levenson J, Biggs AL, Johnson LL, Ameli R, Pine DS, Grillon C (2008) Elevated fear conditioning to socially relevant unconditioned stimuli in social anxiety disorder. Am J Psychiatry 165:124–132.

Liu Y, Huang H, McGinnis-Deweese M, Keil A, Ding M (2012a) Neural substrate of the late positive potential in emotional processing. J Neurosci 32:14563–14572.

Liu Y, Keil A, Ding M (2012b) Effects of emotional conditioning on early visual processing: Temporal dynamics revealed by ERP single‐trial analysis. Hum Brain Mapp 33:909-919.

Liu Y, Murray SO, Jagadeesh B (2009) Time course and stimulus dependence of repetition-induced response suppression in inferotemporal cortex. J Neurophysiol 101:418–436.

Luck SJ (2005) An introduction to the event-related potential technique. Cambridge, MA: MIT Press.

Luo Q, Holroyd T, Jones M, Hendler T, Blair J (2007) Neural dynamics for facial threat processing as revealed by gamma band synchronization using MEG. Neuroimage 34:839–847.

Mayhew SD, Ostwald D, Porcaro C, Bagshaw AP (2013) Spontaneous EEG alpha oscillation interacts with positive and negative BOLD responses in the visual-auditory cortices and default-mode network. Neuroimage 76:362–372.

McGillem CD, Aunon JI, Pomalaza CA (1985) Improved waveform estimation procedures for event-related potentials. IEEE Trans Biomed Eng BME-32, 371–379.

McMahon DBT, Olson CR (2007) Repetition suppression in monkey inferotemporal cortex: relation to behavioral priming. J Neurophysiol 97:3532–3543.

Mitzdorf U (1985) Current source-density method and application in cat cerebral cortex: investigation of evoked potentials and EEG phenomena. Physiol Rev 65:37–100.

Mo J, Liu Y, Huang H, Ding M (2013) Coupling between visual alpha oscillations and default mode activity. Neuroimage 68:112–118.

Mogg K, Millar N, Bradley BP (2000) Biases in eye movements to threatening facial expressions in generalized anxiety disorder and depressive disorder. J Abnorm Psychol 109:695–704.

Moosmann M, Ritter P, Krastel I, Brink A, Thees S, Blankenburg F, Taskin B, Obrig H, Villringer A (2003) Correlates of alpha rhythm in functional magnetic resonance imaging and near infrared spectroscopy. Neuroimage 20:145–158.

Moratti S, Keil A (2005) Cortical activation during Pavlovian fear conditioning depends on heart rate response patterns: an MEG study. Brain Res Cogn Brain Res 25:459–471.

Morris JS, Friston KJ, Büchel C, Frith CD, Young AW, Calder AJ, Dolan RJ (1998a) A neuromodulatory role for the human amygdala in processing emotional facial expressions. Brain 121:47–57.

Morris JS, Friston KJ, Dolan RJ (1998b) Experience-dependent modulation of tonotopic neural responses in human auditory cortex. Proc Biol Sci 265:649–657.

Moratti S, Keil A (2009) Not what you expect: experience but not expectancy predicts conditioned responses in human visual and supplementary cortex. Cereb Cortex 19:2803–2809.

Müller MM, Andersen S, Keil A (2008) Time course of competition for visual processing resources between emotional pictures and a foreground task. Cereb Cortex 18:1892–1899.

Nagai Y, Critchley H, Featherstone E, Fenwick PB, Trimble M, Dolan R (2004) Brain activity relating to the contingent negative variation: an fMRI investigation. Neuroimage 21:1232–1241.

Norris CJ, Chen EE, Zhu DC, Small SL, Cacioppo JT (2004) The interaction of social and emotional processes in the brain. J Cogn Neurosci 16:1818–1829.

Novitskiy N, Ramautar JR, Vanderperren K, De Vos M, Mennes M, Mijovic B, Vanrumste B, Stiers P, Vanden Bergh B, Lagae L, Sunaert S, Van Huffel S, Wagemans J (2011) The BOLD correlates of the visual P1 and N1 in single-trial analysis of simultaneous EEG-fMRI recordings during a spatial detection task. Neuroimage 54:824-835.

O'Doherty J, Rolls ET, Francis S, Bowtell R, McGlone F (2001) Representation of pleasant and aversive taste in the human brain. J Neurophysiol 85:1315–1321.

O'Doherty J, Winston J, Critchley H, Perrett D, Burt D, Dolan R (2003) Beauty in a smile: the role of medial orbitofrontal cortex in facial attractiveness. Neuropsychologia 41:147–155.

Olofsson JK, Nordin S, Sequeira H, Polich J (2008) Affective picture processing: an integrative review of ERP findings. Biol Psychol 77:247–265.

Oya H, Kawasaki H, Howard MA, Adolphs R (2002) Electrophysiological responses in the human amygdala discriminate emotion categories of complex visual stimuli. J Neurosci 22:9502–9512.

Palomba D, Angrilli A, Mini A (1997) Visual evoked potentials, heart rate responses and memory to emotional pictorial stimuli. Int J Psychophysiol 27:55–67.

Pastor MC, Bradley MM, Löw A, Versace F, Moltó J, Lang PJ (2008) Affective picture perception: Emotion, context, and the late positive potential. Brain Res 1189:145–151.

Pearce JM, Hall G (1980) A model for Pavlovian learning: variations in the effectiveness of conditioned but not of unconditioned stimuli. Psychol Rev 87:532–552.

Pessoa L, Adolphs R (2010) Emotion processing and the amygdala: from a "low road" to "many roads" of evaluating biological significance. Nat Rev Neurosci 11:773–783.

Phan KL, Wager T, Taylor SF, Liberzon I (2002) Functional neuroanatomy of emotion: a meta-analysis of emotion activation studies in PET and fMRI. Neuroimage 16:331–348.

Phillips ML, Medford N, Young AW, Williams L, Williams SCR, Bullmore ET, Gray JA, Brammer MJ (2001) Time courses of left and right amygdalar responses to fearful facial expressions. Hum Brain Mapp 12:193–202.

Phillips ML, Young AW, Scott SK, Calder AJ, Andrew C, Giampietro V, Williams SCR, Bullmore ET, Brammer M, Gray JA (1998) Neural responses to facial and vocal expressions of fear and disgust. Proc Biol Sci 265:1809–1817.

Phillips ML, Young AW, Senior C, Brammer M, Andrew C, Calder AJ, Bullmore ET, Perrett DI, Rowland D, Williams SCR, Gray JA, David AS (1997) A specific neural substrate for perceiving facial expressions of disgust. Nature 389:495–498.

Pizzagalli DA, Greischar LL, Davidson RJ (2003) Spatio-temporal dynamics of brain mechanisms in aversive classical conditioning: high-density event-related potential and brain electrical tomography analyses. Neuropsychologia 41:184–194.

Pizzagalli DA, Regard M, Lehmann D (1999) Rapid emotional face processing in the human right and left brain hemispheres: an ERP study. Neuroreport 10:2691–2698.

Pourtois G, Grandjean D, Sander D, Vuilleumier P (2004) Electrophysiological correlates of rapid spatial orienting towards fearful faces. Cereb Cortex 14:619–633.

Quian Quiroga R (2000) Obtaining single stimulus evoked potentials with wavelet denoising. Phys Nonlinear Phenom 145:278–292.

Quian Quiroga R, Garcia H (2003) Single-trial event-related potentials with wavelet denoising. Clin Neurophysiol. 114, 376–390.

Quirk GJ, Armony JL, LeDoux JE (1997) Fear conditioning enhances different temporal components of tone-evoked spike trains in auditory cortex and lateral amygdala. Neuron 19:613–624.

Rajagovindan R, Ding M (2011) From prestimulus alpha oscillation to visual-evoked response: an inverted-U function and its attentional modulation. J Cogn Neurosci 23:1379–1394.

Roberts AC, Tomic DL, Parkinson CH, Roeling TA, Cutter DJ, Robbins TW, Everitt BJ (2007) Forebrain connectivity of the prefrontal cortex in the marmoset monkey (Callithrix jacchus): an anterograde and retrograde tract-tracing study. J Comp Neurol 502:86–112.

Rogers RD, Ramnani N, Mackay C, Wilson JL, Jezzard P, Carter CS, Smith SM (2004) Distinct portions of anterior cingulate cortex and medial prefrontal cortex are activated by reward processing in separable phases of decision-making cognition. Biol Psychiatry 55:594–602.

Romei V, Brodbeck V, Michel C, Amedi A, Pascual-Leone A, Thut G (2008) Spontaneous fluctuations in posterior α-band EEG activity reflect variability in excitability of human visual areas. Cereb Cortex 18:2010–2018.

Romei V, Gross J, Thut G (2010). On the role of prestimulus alpha rhythms over occipito-parietal areas in visual input regulation: correlation or causation? J Neurosci 30:8692–8697.

Rotshtein P, Malach R, Hadar U, Graif M, Hendler T (2001) Feeling or features: different sensitivity to emotion in high-order visual cortex and amygdala. Neuron 32:747–757.

Ruff CC, Bestmann S, Blankenburg F, Bjoertomt O, Josephs O, Weiskopf N, Deichmann R, Driver J (2008). Distinct causal influences of parietal versus frontal areas on human visual cortex: evidence from concurrent TMS–fMRI. Cereb Cortex 18:817–827.

Ruff CC, Blankenburg F, Bjoertomt O, Bestmann S, Freeman E, Haynes JD, Rees G, Josephs O, Deichmann R, Driver J (2006) Concurrent TMS-fMRI and psychophysics reveal frontal influences on human retinotopic visual cortex. Curr Biol 16:1479–1488.

Sabatinelli D, Bradley MM, Fitzsimmons JR, Lang PJ (2005) Parallel amygdala and inferotemporal activation reflect emotional intensity and fear relevance. Neuroimage 24:1265–1270.

Sabatinelli D, Bradley MM, Lang PJ, Costa VD, Versace F (2007a) Pleasure rather than salience activates human nucleus accumbens and medial prefrontal cortex. J Neurophysiol 98:1374–1379.

Sabatinelli D, Keil A, Frank DW, Lang PJ (2013) Emotional perception: correspondence of early and late event-related potentials with cortical and subcortical functional MRI. Biol Psychol 92:513-519.

Sabatinelli D, Lang PJ, Bradley MM, Costa VD, Keil A (2009) The timing of emotional discrimination in human amygdala, inferotemporal, and occipital cortex. J Neurosci 29:14864-14868.

Sabatinelli D, Lang PJ, Keil A, Bradley MM (2007b) Emotional perception: correlation of functional MRI and event-related potentials. Cereb Cortex 17:1085 –1091.

Sakai K (2008) Task set and prefrontal cortex. Annu Rev Neurosci 31:219–245.

Sauseng P, Feldheim JF, Freunberger R, Hummel FC (2011) Right prefrontal TMS disrupts interregional anticipatory EEG alpha activity during shifting of visuospatial attention. Front Psychol 2:241.

Sauseng P, Klimesch W, Stadler W, Schabus M, Doppelmayr M, Hanslmayr S, Gruber WR, Birbaumer N (2005). A shift of visual spatial attention is selectively associated with human EEG alpha activity. Eur J Neurosci 22:2917–2926.

Scheeringa R, Mazaheri A, Bojak I, Norris DG, Kleinschmidt A (2011) Modulation of visually evoked cortical fMRI responses by phase of ongoing occipital alpha oscillations. J Neurosci 31:3813 –3820.

Schupp HT, Cuthbert BN, Bradley MM, Cacioppo JT, Ito T, Lang PJ (2000) Affective picture processing: the late positive potential is modulated by motivational relevance. Psychophysiology 37:257–261.

Schupp HT, Cuthbert B, Bradley M, Hillman C, Hamm A, Lang P (2004a) Brain processes in emotional perception: motivated attention. Cogn Emot 18:593–611.

Schupp HT, Junghöfer M, Weike AI, Hamm AO (2004b) The selective processing of briefly presented affective pictures: an ERP analysis. Psychophysiology 41:441–449.

Schupp HT, Markus J, Weike AI, Hamm AO (2003) Emotional facilitation of sensory processing in the visual cortex. Psychol Sci 14:7 –13.

Schwabe L, Obermayer K (2005) Adaptivity of tuning functions in a generic recurrent network model of a cortical hypercolumn. J Neurosci 25:3323–3332.

Shulman GL, McAvoy MP, Cowan MC, Astafiev SV, Tansy AP, D'Avossa G, Corbetta M (2003) Quantitative analysis of attention and detection signals during visual search. J Neurophysiol 90:3384–3397.

Shulman GL, Ollinger JM, Akbudak E, Conturo TE, Snyder AZ, Petersen SE, Corbetta M (1999) Areas involved in encoding and applying directional expectations to moving objects. J Neurosci 19:9480–9496.

Stolarova M, Keil A, Moratti S (2006) Modulation of the C1 visual event-related component by conditioned stimuli: evidence for sensory plasticity in early affective perception. Cereb Cortex 16:876 –887.

Straube T, Miltner WHR (2011) Attention to aversive emotion and specific activation of the right insula and right somatosensory cortex. Neuroimage 54:2534–2538.

Tang AC, Sutherland MT, McKinney CJ (2005) Validation of SOBI components from high-density EEG. Neuroimage 25:539–553.

Thut G, Nietzel A, Brandt SA, Pascual-Leone A (2006). α-band electroencephalographic activity over occipital cortex indexes visuospatial attention bias and predicts visual target detection. J Neurosci 26:9494–9502.

Tolias AS, Keliris GA, Smirnakis SM, Logothetis N (2005) Neurons in macaque area V4 acquire directional tuning after adaptation to motion stimuli. Nat Neurosci 8:591–593.

Truccolo WA, Ding M, Knuth KH, Nakamura R, Bressler SL (2002) Trial-to-trial variability of cortical evoked responses: implications for the analysis of functional connectivity. Clin Neurophysiol 113:206–226.

Truccolo W, Knuth KH, Shah A, Bressler SL, Schroeder CE, Ding M (2003) Estimation of single-trial multicomponent ERPs: differentially variable component analysis (dVCA). Biol Cybern 89:426–438.

Tuan PD, Möcks J, Köhler W, Gasser T (1987) Variable latencies of noisy signals: estimation and testing in brain potential data. Biometrika 74:525–533.

Vanderperren K, De Vos M, Ramautar JR, Novitskiy N, Mennes M, Assecondi S, Vanrumste B, Stiers P, Van den Bergh BRH, Wagemans J, Lagae L, Sunaert S, Van Huffel S (2010) Removal of BCG artifacts from EEG recordings inside the MR scanner: A comparison of methodological and validation-related aspects. Neuroimage 50:920–934.

Vossel S, Weidner R, Driver J, Friston KJ, Fink GR (2012) Deconstructing the architecture of dorsal and ventral attention systems with dynamic causal modeling. J Neurosci 32:10637–10648.

Vuilleumier P, Armony JL, Driver J, Dolan RJ (2001) Effects of attention and emotion on face processing in the human brain: an event-related fMRI study. Neuron 30:829–841.

Walsh BJ, Buonocore MH, Carter CS, Mangun GR (2010) Integrating conflict detection and attentional control mechanisms. J Cogn Neurosci 23:2211–2221.

Wang X, Chen Y, Ding M (2008) Estimating Granger causality after stimulus onset: a cautionary note. Neuroimage 41:767–776.

Wang X, Ding M (2011) Relation between P300 and event-related theta-band synchronization: a single-trial analysis. Clin Neurophysiol 122:916–924.

Weinberger NM (1995) Dynamic regulation of receptive fields and maps in the adult sensory cortex. Annu Rev Neurosci 18:129–158.

Weinberger NM (2004) Specific long-term memory traces in primary auditory cortex. Nat Rev Neurosci 5:279–290.

Weinberg A, Hajcak G (2011) Electrocortical evidence for vigilance-avoidance in generalized anxiety disorder. Psychophysiology 48:842–851.

Wen X, Yao L, Liu Y, Ding M (2012) Causal interactions in attention networks predict behavioral performance. J Neurosci 32:1284–1292.

Weymar M, Schwabe L, Löw A, Hamm AO (2012) Stress sensitizes the brain: increased processing of unpleasant pictures after exposure to acute stress. J Cogn Neurosci 24:1511–1518.

Whalen PJ, Rauch SL, Etcoff NL, McInerney SC, Lee MB, Jenike MA (1998) Masked presentations of emotional facial expressions modulate amygdala activity without explicit knowledge. J Neurosci 18:411–418.

Wills AJ (2009) Prediction errors and attention in the presence and absence of feedback. Curr Dir Psychol Sci 18:95–100.

Wills AJ, Lavric A, Croft GS, Hodgson TL (2007) Predictive learning, prediction errors, and attention: Evidence from eventrelated potentials and eye tracking. J Cogn Neurosci 19:843–854.

Woody C (1967) Characterization of an adaptive filter for the analysis of variable latency neuroelectric signals. Med Biol Eng 5:539–554.

Worden MS, Foxe JJ, Wang N, Simpson GV (2000) Anticipatory biasing of visuospatial attention indexed by retinotopically specific α-band electroencephalography increases over occipital cortex. J Neurosci 20, RC63.

Xu L, Stoica P, Li J, Bressler SL, Shao X, Ding M (2009) ASEO: a method for the simultaneous estimation of single-trial eventrelated potentials and ongoing brain activities. IEEE Trans Biomed Eng 56:111–121.

Yamagishi N, Callan DE, Goda N, Anderson SJ, Yoshida Y, Kawato M (2003) Attentional modulation of oscillatory activity in human visual cortex. Neuroimage 20:98–113.

Zald DH (2003) The human amygdala and the emotional evaluation of sensory stimuli. Brain Res Rev 41:88–123.

Zhang Y, Ding M (2010) Detection of a weak somatosensory stimulus: role of the prestimulus mu rhythm and its top-down modulation. J Cogn Neurosci 22:307–322.

BIOGRAPHICAL SKETCH

Yuelu Liu was born in 1985, in city of Changsha, Hunan province, China. He graduated from the middle school attached to the Hunan Normal University in 2003. He did his undergraduate study at Beijing Institute of Technology and earned the B.S. degree in electrical and information engineering in 2007. He then enrolled in the graduate program at the University of Florida and earned his M.S. degree in electrical engineering in 2009. During his graduate study, Yuelu became interested in human cognitive neuroscience and continued to pursue his doctoral degree in the J Crayton Pruitt Family Department of Biomedical Engineering under the mentorship of Dr. Mingzhou Ding. He received his Ph.D. degree from the University of Florida in the summer of 2013. His current research interests mainly include applying multimodal imaging and advanced engineering methods to understand the neural mechanisms underlying higher-level human cognitive functions such as attention and emotion and their impairments in neurological and psychiatric disorders.